Mucosal-associated invariant T (MAIT) cells mediate protective host responses in sepsis.

Shubhanshi Trivedi,[1] Daniel Labuz,[1] Cole P. Anderson,[1] Claudia V. Araujo,[6] Antoinette Blair,[6] Elizabeth A. Middleton,[2] Owen Jensen,[1] Alexander Tran,[4] Matthew A. Mulvey,[4] Robert A. Campbell,[6] J. Scott Hale,[4] Matthew T. Rondina,[3,5,6,7] Daniel T. Leung,[1,4,7]

[1]Division of Infectious Disease, [2]Division of Pulmonary and Critical Care, [3]Division of General Internal Medicine, Department of Internal Medicine; [4]Division of Microbiology and Immunology, Department of Pathology; [5]George E. Wahlen VAMC Department of Internal Medicine and GRECC; [6]Molecular Medicine Program, University of Utah, Salt Lake City, Utah

[7]co-senior authors

Corresponding author:

Daniel T Leung, M.D.

Address: 26 North Medical Drive, Salt Lake City, UT 84132, USA

Telephone: 801-581-8804

Fax: 801-585-3377

Email: daniel.leung@utah.edu

Conflict of interests: The authors have declared that no conflict of interest exists.

Abstract

Sepsis is a systemic inflammatory response to infection and a leading cause of death. Mucosal-associated invariant T (MAIT) cells are innate-like T cells enriched in mucosal tissues that recognize bacterial ligands. We investigated MAIT cells during clinical and experimental sepsis, and their contribution to host responses. In experimental sepsis, MAIT-deficient mice had significantly increased mortality and bacterial load, and reduced tissue-specific cytokine responses. MAIT cells of WT mice expressed lower levels of IFN-γ and lL-17a during sepsis compared to sham surgery, changes not seen in non-MAIT T cells. MAIT cells of patients at sepsis presentation were significantly reduced in frequency compared to healthy donors, and were more activated, with decreased IFN-γ production, compared to both healthy donors and paired 90-day samples. Our data suggest that MAIT cells are highly activated and become dysfunctional during clinical sepsis, and contribute to tissue-specific cytokine responses that are protective against mortality during experimental sepsis.

Introduction

Sepsis is a life threatening syndrome caused by dysregulated host responses to infection resulting in organ dysfunction (1). It is a leading cause of death worldwide, accounting for 5.3 million deaths annually (2). Sepsis is characterized by a systemic acute pathologic hyper-inflammatory response and an opposing anti-inflammatory response that can occur concurrently (3). Hallmarks of sepsis include a decreased ability to eliminate primary pathogens and an increased susceptibility to secondary nosocomial infections (4). In addition, it is associated with a protracted immunosuppressed state that contributes to morbidity and mortality (5). Unfortunately, clinical trials over the past 3 decades of interventions targeting the hyper-inflammatory state of sepsis have largely failed to consistently improve clinical outcomes (6-8), and effective treatments are needed.

Many components of host responses are altered during sepsis, including activation of innate effector cells such as platelets, neutrophils, epithelial cells, and endothelial cells. In some settings, cellular activation is associated with dysfunctional responses and adverse clinical outcomes. Studies on immunosuppression in sepsis have largely focused on exhaustion, apoptosis, and reprogramming of a broader range of effector cells, including T cells, B cells, neutrophils, and other antigen-presenting cells (9). Unconventional T cells, such as invariant NKT (iNKT) cells, γδ T cells, and mucosal-associated invariant T (MAIT) cells, bridge the innate and adaptive arms of the immune response, and have the capacity to contribute to both early-phase inflammation and late-phase immunosuppression.

MAIT cells are innate-like T cells restricted by MHC-related molecule 1 (MR1) and MAIT ligands belong to a class of transitory intermediates of the riboflavin synthesis pathway (10). They express an invariant T cell receptor (TCR) TRAV1-2 (or Vα7.2) in humans and TRAV-1 (or Vα19) in mice and a variable, but restricted, number of TRAJ and TCR β chains. MAIT cells are abundant in mucosal tissues such as the liver, lung, and mesenteric lymph nodes and gut lamina propria. In humans, they constitute 1-10% of peripheral blood T lymphocytes, up to 10% of intestinal T cells, and up to 40% of T cells in the liver (11, 12). Recent studies have highlighted the protective role of MAIT cells in host antibacterial responses *in vivo* (13-15). It has also been shown that in patients with sepsis, MAIT cell frequencies are decreased in circulation compared to healthy control donors and uninfected critically-ill patients (16). Septic patients with persistent MAIT cell depletion also have a higher incidence of secondary, ICU-acquired infections (16). However, detailed phenotypic and functional MAIT cell changes during sepsis, as well as the mechanisms by which MAIT cells contribute to host immune responses in sepsis, are not known. In this work, we used complementary, longitudinal studies in sepsis patients and in a relevant murine sepsis model to study the role of MAIT cells in sepsis pathology. We examined immune responses in C57BL/6 wild type (WT) or MR1 knock-out (*Mr1*$^{-/-}$; i.e. MAIT depleted) mice using the cecal ligation and puncture (CLP) model of polymicrobial sepsis. Additionally, we evaluated the phenotype and function of human MAIT cells during acute sepsis and at 3 months after sepsis.

Results

MAIT cells have decreased expression of effectors during experimental sepsis.

To assess MAIT cell effector function during sepsis, we examined MAIT cells in the lungs of WT mice undergoing CLP, a polymicrobial model of sepsis, or sham surgery. We chose lungs given the frequent association of lung injury with clinical sepsis (17, 18), and because it is among the most abundant site of MAIT cells in mice (19). While we noted similar frequencies of MR1-5OP-RU-tetramer$^+$ (from here on, referred to as MR1-tetramer$^+$) MAIT cells in CLP mice as in sham mice (Figure 1A and B), we found in sorted MAIT cells that gene expression of MAIT effectors *Ifng* (P = 0.04) and *Il17a* (P = 0.02) were significantly lower (and *GzmB* trended lower, P = 0.14) in septic mice compared to sham mice (Figure 1C). Conversely, in non-MAIT TCRβ$^+$CD3$^+$ T cell populations, *Ifng* (P = 0.06)*, Il17a* (P = 0.16) and *Gzmb* (P = 0.49) mRNA expression levels were similar between septic mice and sham mice (Figure 1D).

To further confirm that MAIT cell effector function is impaired during experimental sepsis, we evaluated IFNγ, TNFα, IL-17a, GM-CSF and IL-10 protein expression in MAIT cells of lung tissue using flow cytometry. We found that similar to *Ifng* mRNA expression, percentage frequencies of MAIT cells expressing IFNγ were significantly lower (P = 0.04) in septic mice compared to sham mice (Figure 2A). Mean fluorescent intensity (MFI) of IFNγ staining in TCRβ$^+$ MR1-5OP-RU-tetramer$^+$ MAIT cells was also significantly reduced (P = 0.02) in septic mice compared to sham mice (Figure 2B). Conversely, in non-MAIT TCRβ$^+$CD3$^+$ T cell populations, IFNγ protein expression was significantly higher (P = 0.0005) in septic mice compared to sham mice (Figure 2C). No

104 significant differences were observed in IFNγ expression in *i*NKT and TCRγδ cells
105 (Figure 2D and E). No significant differences were observed in frequencies of TNFα, IL-
106 17a, GM-CSF and IL-10 between the groups.
107
108 **MAIT deficiency increases bacterial burden and mortality during experimental**
109 **sepsis.**
110 We examined whether the absence of MAIT cells altered survival outcomes *in vivo*
111 during experimental sepsis. In the CLP model of polymicrobial sepsis (20, 21), we saw
112 that MR1-deficient mice (*Mr1*$^{-/-}$) which lack MAIT cells, had significantly increased
113 sepsis-related mortality compared to WT mice (Figure 3A). The majority (11/15, ~73%)
114 of *Mr1*$^{-/-}$ mice died 24 to 48 hours following induction of sepsis, while the majority (13/15,
115 ~87%) of WT mice survived up to 100 hours after sepsis (Figure 3A). On examining
116 bacterial counts 18 hours following CLP, we found that *Mr1*$^{-/-}$ mice had a significantly
117 higher burden of bacteria in blood compared to WT mice (Figure 3B). The microbiota
118 associated with *Mr1*$^{-/-}$ mice may differ from wild-type mice (22); therefore, we examined
119 whether such differences affect susceptibility to sepsis. In experiments in which bedding
120 was transferred between *Mr1*$^{-/-}$ and WT cages (23) prior to CLP, we found that *Mr1*$^{-/-}$
121 mice had significantly increased mortality compared to WT mice (Figure 3C). To extend
122 these findings to a setting of sepsis due to a single pathogen, we induced sepsis via
123 intraperitoneal injection of a clinical strain of extraintestinal pathogenic *Escherichia coli*
124 (ExPEC). As we observed in the CLP, polymicrobial model of sepsis, *Mr1*$^{-/-}$ mice had
125 significantly higher mortality from ExPEC sepsis, compared to WT mice (Figure 3-figure
126 supplement 1).

MAIT deficiency is associated with reduced lung cytokine responses in experimental sepsis.

To determine the contribution of MAIT cells to sepsis-induced tissue inflammatory responses, we evaluated MAIT-associated cytokines (24) in lung homogenates after CLP. Compared to WT mice, *Mr1*$^{-/-}$ mice had significantly reduced levels of lung IFN-γ, TNFα, IL-17A, IL-10 and GM-CSF: cytokines produced by MAIT cells (24) (Figure 4). Interestingly, serum, liver and gut cytokines were less affected than lung cytokines in *Mr1*$^{-/-}$ mice following sepsis (Figure 4- figure supplement 1-3).

MAIT deficiency is associated with reduced tissue-specific interstitial macrophages and monocytic dendritic cell frequencies.

MAIT cells can contribute to cytokine release from macrophages (25) and have shown to promote inflammatory monocyte differentiation into dendritic cells during pulmonary infection (26). Thus, we next sought to determine the cause of reduced tissue cytokine production of *Mr1*$^{-/-}$ mice during sepsis. We approached this by determining how an absence of MAIT cells influences the frequencies of lung innate immune cells, including alveolar macrophages (AMs), interstitial macrophages (IMs), monocytic dendritic cells (moDCs) and plasmocytoid DCs (pDCs). As compared to WT mice, *Mr1*$^{-/-}$ mice had a significantly lower proportion of IMs (Siglec-F^{-} CD24^{-} MHCII^{+} CD11c^{+} CD11b^{+} CD64^{+} cells; Figure 5A) and moDCs (Siglec-F^{-} MHCII^{+} CD11c^{+} CD11b^{+} Ly-6C^{+} cells; Figure 5B) following CLP. Loss of MAIT cells did not influence AMs, pDCs or neutrophils, however, following CLP (Figure 5C -E). To investigate the possible mechanism by

which MAIT cells are protective, we performed *ex vivo* expansion of lung MAIT cells from WT mice using 5-OP-RU/MR1 artificial antigen presenting cells (27) and co-cultured them with $Ly6C^+$ $CD11b^+$ monocytes, also isolated from WT mice, for 18 hours. We found significantly higher amounts of IFNγ (Figure 5-figure supplement 1A) and GM-CSF (Figure 5-figure supplement 1B) in co-cultures stimulated with 5-amino-6-D-ribitylaminouracil (5-A-RU) and methylglyoxal (MeG) (28) compared to unstimulated and monocyte only controls indicating that MAIT cells in lung can interact with monocytes to produce effector cytokines.

We next examined whether loss of MAIT cells altered the frequencies of other unconventional T cells such as invariant natural killer T cells (*i*NKT) (29, 30) and γδ T cells (31, 32) in sepsis. We observed that frequencies of *i*NKT and γδ T cells in lungs were reduced during sepsis, consistent with prior studies showing that frequencies of *i*NKT (29, 30) and γδ T cells (31, 32) are modulated in response to polymicrobial sepsis. However, there were no differences in frequencies of *i*NKT or γδ T cells between *Mr1*$^{-/-}$ and WT mice (Figure 5-figure supplement 2).

Consistent with murine sepsis studies, MAIT cell frequency, activation, and effectors are altered in septic patients.

We examined MAIT cells isolated from the blood of 33 septic patients (16 female and 17 male, mean age 59 +/- 2.7years, mean SOFA score 4.6) within 48 (± 24) hours of ICU admission for sepsis (day 1, D1). In 12 of these same patients (6 female and 6 male, mean age 60.5 +/- 4 years), we repeated MAIT phenotyping again approximately 90

days after their ICU admission for sepsis. We compared them to 21 age- and sex-matched healthy donors (HD) (10 female and 11 male, mean age 51 +/- 3.8 years). The identified causes of sepsis included pneumonia, urinary tract, intra-abdominal, and soft-tissue infections. Upon ICU admission, septic patients showed lower frequencies of MR1-tetramer^{+} MAIT cells within the T cell (CD3^{+}) compartment compared to healthy donors (HD) (Figure 6, A and B). At 90 days after sepsis, MAIT cell frequencies were not statistically different from day 1 septic patients and HD (Figure 6B and C).

Next, we evaluated markers of MAIT cell activation, exhaustion, and intracellular cytokine expression in a subset of surviving septic patients and for which paired samples at both Day 1 and Day 90 were available (n=12). Upon ICU admission (Day 1), the expression of MAIT cell activation markers, including CD69, CD38, and CD137, was significantly higher in septic patients compared to HD (Figure 6D). However, when assessed again in these same septic patients on Day 90, the expression of MAIT cell activation markers had returned to levels comparable to HD (Figure 6D). Upon ICU admission, we also found a higher expression of TIM-3 (P = 0.03), and LAG-3 (trend with P = 0.14), inhibitory receptors associated with T cell exhaustion, in MAIT cells of septic patients compared to HD (Figure 6E). As with MAIT cell activation markers, exhaustion markers LAG-3 and TIM-3 in septic patients at Day 90 had returned to levels similar to that of HD (Figure 6E). Of note, PD-1 expression was lower (but not statistically significant, P = 0.11) in septic patients compared to HD (Figure 6E).

We then examined MAIT cell effector functions by analyzing the intracellular expression of MAIT-associated inflammatory cytokines (IFN-γ, IL-17 and TNF-α) and granzyme B after *ex vivo* TCR stimulation using *E. coli* (33). Upon ICU admission, MAIT cells from septic patients showed significantly less IFN-γ production after *E. coli* stimulation, compared with HD. As with MAIT cell activation and exhaustion markers, IFN-γ production returned to levels comparable with HD at Day 90 (Figure 7A). No significant differences were observed in IL-17 (Figure 7B), TNF-α (Figure 7C) and granzyme B (Figure 7D) expression in MAIT cells among the groups.

Overall, these data demonstrate that during clinical sepsis, MAIT cell frequencies are lower, highly activated, and less capable of mounting IFN-γ responses upon stimulation. Moreover, at 90 days following sepsis, MAIT cell activation and IFN-γ responses have returned to levels comparable with matched HD.

Discussion

Recent reports provide evidence that MAIT cells play an important role in antibacterial responses (34, 35). Despite this, very little is known about this unconventional T cell in sepsis. Our study reveals major alterations in activation, function, and dysfunction of MAIT cells in both clinical and experimental models of sepsis. We show that acutely during clinical sepsis, MAIT cells are highly activated, lower in frequency, and have an altered functional phenotype evidenced by reduced IFN-γ cytokine expression. Moreover, at 90 days after sepsis, these changes in MAIT cells have resolved as compared to matched healthy subjects. Using relevant animal models of sepsis, we show similarly that tissue-resident MAIT cells are dysfunctional during sepsis. Moreover, our experimental data indicate that MAIT cells are protective during sepsis, as a deficiency of MAIT cells resulted in significantly higher bacterial burden and mortality. These results indicate that despite being rendered dysfunctional, MAIT cells may augment host immune responses and therefore outcomes during sepsis.

In both a polymicrobial model of sepsis (*i.e.* CLP) and a monomicrobial model using a clinical isolate of ExPEC, we found that MAIT-deficient (*Mr1*$^{-/-}$) mice have higher mortality, and that this is associated with a higher bacterial burden. Our experimental data from the ExPEC model of sepsis, as well as from experiments where bedding was transferred between *Mr1*$^{-/-}$ and WT mice, suggest that the differences in mortality observed with CLP are unlikely to be due to differences in the microbiota. We also found that *Mr1*$^{-/-}$ mice had lower levels of tissue cytokines (IFN-γ, TNF-α, IL-17, GM-CSF) than that in WT mice following induction of sepsis. We hypothesize that MAIT

cells plays a protective role against sepsis pathology by regulating cytokine expression and maintaining a balance in immune response following sepsis to minimize tissue injury. As MAIT cells are capable of bridging the innate and adaptive immune systems, it has also been postulated that their actions are mediated in part by their interaction with macrophages or monocyte-derived dendritic cells. Interestingly, we found that in sepsis, MAIT-deficient mice produce less GM-CSF and have lower frequencies of lung interstitial macrophages and monocytic dendritic cells compared to WT mice. These observations are concordant with previous work demonstrating MAIT cell promotion of early pulmonary GM-CSF production, and differentiation of inflammatory monocytes into moDCs during pulmonary infection (26). Our co-culture experiments showing that MAIT cells produce higher amounts of GM-CSF upon stimulation with the MAIT ligand 5-A-RU further confirms this hypothesis. Further work to examine whether tissue-resident MAIT cells have protective effects against sepsis pathology is warranted.

Our finding of decreased MAIT cell frequencies during severe sepsis are consistent with a previous study demonstrating that MAIT cells are decreased in patients with severe sepsis, a decrease that was not seen in other T cell populations examined, including *i*NKT and γδ T cells, suggesting cell-specific, rather than global, depletion (16). To extend this work, we found that at approximately 90 days after sepsis MAIT cell frequencies had returned to similar levels observed in matched healthy donors. Furthermore, we found that MAIT cells express elevated levels of activation markers in septic patients, and that these markers also return to similar levels as in healthy donors following recovery from sepsis. The depletion of MAIT cells from circulation in septic

patients is similar to what has been observed in other infections (36) (37) (38), and may be a result of apoptotic cell death, TCR internalization, or migration to peripheral tissues, although the underlying mechanisms remain to be elucidated.

Previous work had shown an association of MAIT cell frequency with protection against secondary infection in the ICU (16). In this study, we found that in D1 sepsis patients, *ex-vivo* stimulated MAIT cells had a depressed IFN-γ response compared to healthy donors and patients reassessed 90 days following admission for sepsis. A similar decrease in IFN-γ response was also seen in MAIT cells in the lung tissue of mice undergoing CLP compared to mice undergoing sham surgery. Together with an increase in expression of co-inhibitory receptors on human MAIT cells, our data suggest that during clinical sepsis, MAIT cells are dysfunctional. This may prevent MAIT cells from mounting an optimal response against microbial pathogens, a hypothesis consistent with our experimental data indicating that loss of MAIT cells results in increased bacterial burden and mortality during sepsis. Previous work has shown that superantigens from bacterial pathogens such as *Staphylococcus spp.* and *Streptococcus spp.* can directly trigger rapid activation of MAIT cells to mount IFN-γ, TNF-α, and IL-2 responses in an MR1-independent manner (37), and that MAIT cells primed by superantigens are exhausted and anergic to cognate antigens such as *E.coli*.

Our study has a number of limitations. Firstly, our co-culture experiments demonstrating the production of GM-CSF by ligand stimulation of expanded lung MAIT cells in presence of lung monocytes were performed *ex vivo*. Further experiments on the

protective role of MAIT-derived GM-CSF during sepsis are needed. Secondly, our study of patients was not powered to detect differences in MAIT cells between causes of sepsis. Larger studies are needed to examine differences in MAIT cell activity and function between different causes. Lastly, our experiments demonstrated decreases in lung interstitial macrophages and monocytes, along with GM-CSF production, are associated with response to CLP in *Mr1*$^{-/-}$ mice. But whether these deficient responses resulted in increased lung injury remains to be investigated further.

In conclusion, we demonstrate that MAIT cells undergo functional and phenotypic changes during clinical and experimental sepsis. We found that MAIT deficient mice have higher microbial burden, lower tissue cytokine production, and higher mortality during sepsis. Despite this dysfunction, our data provide new insights into the potential protective role of MAIT cells, and their contribution towards tissue-specific cytokine responses, during sepsis. Defining MAIT cells as a critical therapeutic target during sepsis, and defining the mechanisms that regulate MAIT cell function, will potentially enable the development of novel translational strategies targeted to enhance MAIT cell functionality to improve outcomes in sepsis.

298 **Materials and methods**

Key Resources Table				
Reagent type (species) or resource	**Designation**	**Source or reference**	**Identifiers**	**Additional information**
Antibody	FITC anti-mouse CD3 antibody (rat monoclonal)	Biolegend	Cat# 100203	(1:50)
Antibody	Brilliant Violet 510™ anti-mouse NK-1.1 (mouse monoclonal)	Biolegend	Cat# 108738	(1:50)
Antibody	BV711 anti-mouse CD49b (hamster monoclonal)	BD	Cat# 740704	(1:100)
Antibody	PE/Cyanine7 anti-mouse TCR γ/δ (hamster monoclonal)	Biolegend	Cat# 118123	(1:100)
Antibody	BV421 anti-mouse TCRβ (hamster monoclonal)	Biolegend	Cat# 109229	(1:100)
Antibody	PE/Cyanine5 anti-mouse/human CD45R/B220 (rat monoclonal)	Biolegend	Cat# 103209	(1:100)
Antibody	Brilliant Violet 650™ anti-mouse/human CD44 (rat monoclonal)	Biolegend	Cat# 103049	(1:100)
Antibody	Alexa Fluor® 700 anti-mouse CD45 (rat monoclonal)	Biolegend	Cat# 103127	(1:200)

Antibody	FITC anti-mouse/human CD11b (rat monoclonal)	Biolegend	Cat# 101205	(1:200)
Antibody	PE/Cyanine7 anti-mouse CD11c (hamster monoclonal)	Biolegend	Cat# 117317	(1:100)
Antibody	BV711 anti-mouse Siglec-F (rat monoclonal)	BD	Cat# 740764	(1:100)
Antibody	Brilliant Violet 605™ anti-mouse CD64 (FcγRI) (mouse monoclonal)	Biolegend	Cat# 139323	(1:50)
Antibody	PE anti-mouse CD24 (rat monoclonal)	Biolegend	Cat# 101807	(1:100)
Antibody	PerCP/Cyanine5.5 anti-mouse Ly-6G (rat monoclonal)	Biolegend	Cat# 127616	(1:100)
Antibody	BV510 anti-mouse CD103 (hamster monoclonal)	Biolegend	Cat# 121423	(1:50)
Antibody	APC anti-mouse CD86 (rat monoclonal)	Biolegend	Cat# 105011	(1:100)
Antibody	PE/Dazzle™ 594 anti-mouse Ly-6C (rat monoclonal)	Biolegend	Cat# 128043	(1:100)
Antibody	Brilliant Violet 421™ anti-mouse I-A/I-E (rat monoclonal)	Biolegend	Cat# 107631	(1:100)
Antibody	Alexa Fluor® 700 anti-human CD137 (4-1BB) (mouse monoclonal)	Biolegend	Cat# 309816	(1:100)

Antibody	BUV395 Mouse Anti-Human CD3	BD	Cat# 563548	(1:200)
Antibody	Anti-human CD8 Monoclonal Antibody (3B5), PE-Cyanine5.5	ThermoFisher Scientific	Cat# MHCD0818	(1:200)
Antibody	BUV496 Mouse Anti-Human CD4	BD	Cat# 612937	(1:100)
Antibody	Brilliant Violet 711™ anti-human TCR Vα7.2 (mouse monoclonal)	Biolegend	Cat# 351731	(1:50)
Antibody	Brilliant Violet 785™ anti-human CD223 (LAG-3) (mouse monoclonal)	Biolegend	Cat# 369321	(1:50)
Antibody	Brilliant Violet 650™ anti-human CD25 (mouse monoclonal)	Biolegend	Cat# 302633	(1:100)
Antibody	Brilliant Violet 605™ anti-human CD279 (PD-1) (mouse monoclonal)	Biolegend	Cat# 329923	(1:100)
Antibody	Brilliant Violet 510™ anti-human CD161 (mouse monoclonal)	Biolegend	Cat# 339921	(1:100)
Antibody	PE/Cyanine5 anti-human CD69 (mouse monoclonal)	Biolegend	Cat# 310907	(1:100)
Antibody	FITC anti-human HLA-DR	Biolegend	Cat# 980402	(1:50)
Antibody	Brilliant Violet 421™ anti-human CD366 (Tim-3) (mouse monoclonal)	Biolegend	Cat# 345007	(1:50)

Antibody	PE/Cyanine7 anti-human CD38 (mouse monoclonal)	Biolegend	Cat# 303515	(1:100)
Antibody	FITC anti-human IL-17A Antibody (mouse monoclonal)	Biolegend	Cat# 512303	(1:100)
Antibody	PE/Cyanine7 anti-human IFN-γ (mouse monoclonal)	Biolegend	Cat# 502527	(1:200)
Antibody	Anti–human TNF alpha Monoclonal Antibody (MAb11), eFluor 450	ThermoFisher Scientific	Cat# 48-7349-42	(1:100)
Antibody	Alexa Fluor® 700 anti-human/mouse Granzyme B	Biolegend	Cat# 372221	(1:100)

Mice

10-14 weeks old male C57BL/6J wild type mice were obtained from Jackson laboratories and *Mr1*$^{-/-}$ mice, which were back-crossed to the C57BL/6N background (10 generations) and then the C57BL/6J background (10 generations) (22), were obtained from Siobhan Cowley (US FDA). All mice were bred in pathogen-free facility at the University of Utah. The animals were kept at a constant temperature (25°C) with unlimited access to pellet diet and water in a room with a 12 h light/dark cycle. All animals were monitored daily and infected animals were scored for the signs of clinical illness severity as previously described (20). Animals were ethically euthanized using CO_2.

Mouse models of sepsis

C57BL/6 mice were anesthetized with ketamine/xylazine (100 mg/kg and 10 mg/kg, i.p., respectively), and sepsis was induced by cecum ligation and puncture (CLP) as previously described (Hubbard et al., 2005). After surgery, the animals received subcutaneous sterile isotonic saline (1 mL) for fluid resuscitation. Sham-operated mice were subjected to identical procedures except that CLP was not done. The animals were followed for 5 days after the surgical procedure for determination of survival. Bacterial loads were determined by serial dilution and plating of lung homogenates and blood on LB agar plates.

To examine monomicrobial sepsis, mice were injected intraperitoneally with 200 µl of PBS containing ~1x10^6 cfu of Extraintestinal pathogenic *Escherichia coli* (ExPEC) clinical strain F11 (39). Bacteria (F11) was grown from frozen stocks in static modified M9 media at 37°C for 24 hours prior to use in the sepsis model. Mice were monitored for 5 days for determination of survival.

Bedding transfer procedure

Bedding transfer procedure was followed as previously described (23). Briefly, bedding transfers were performed among *Mr1*$^{-/-}$ cages and WT cages. Bedding was mixed at 3–4 days and at 8–10 days following these cage changes (as fresh bedding is provided every 14 days, this represents bedding transfers performed twice within each two-week cycle). At each of these time points, roughly one-quarter of soiled bedding was collected from each cage and the bedding from all cages was mixed in an autoclaved sterile container, followed by redistribution across all cages. Soiled bedding was collected and

mixed within a freshly cleaned biological safety cabinet within the room where animals were housed. After 4-5 weeks of bedding transfers, polymicrobial sepsis was induced using CLP.

Lung mononuclear cell isolation

For lung digestion and preparation of single cell suspensions, lungs were perfused using sterile phosphate-buffered saline. After removal, the lung dissociation protocol (Miltenyi Biotec, Bergisch Gladbach, Germany) was performed using the mouse Lung Dissociation Kit (Miltenyi Biotec) and the gentleMACS Dissociator (Miltenyi Biotec) as per manufacturer's instructions. After dissociation, cells were passed through a 70 µm cell strainer and washed with RPMI with 10 % FBS. Red blood cells were lysed with red blood cell lysis buffer. Lung mononuclear cells were then washed twice in RPMI with 10 % FBS before use in subsequent experiments.

Tetramer and surface-staining of lung single cell suspensions

From each group of animals, 1-2 million cells aliquots were prepared and to exclude dead cells from analysis cells were first stained with the fixable viability dye eFluor™ 780 (eBioscience) for 15 min. at room temperature (RT). Cells were incubated with anti-mouse CD16/CD32 Fc Block antibody (BD Biosciences, USA), for 20 min at 4 °C. Cells were then stained for 30 min at RT with appropriately diluted PE conjugated 5-OP-RU-loaded species-specific MR1-tetramers or α-GalCer (PBS-44)–loaded CD1d tetramer conjugated to APC, anti-CD3-FITC (Biolegend), anti-CD161-BV510 (Biolegend), anti-CD49b-BV711 (BD), anti-TCRγδ-PE-Cy7 (Biolegend), anti-TCRβ-BV421 (Biolegend),

anti-CD45R-PE-Cy5 and anti-CD44-BV650 (Biolegend). To evaluate different antigen presenting cells, after Fc Block incubation, cells were also surface stained with anti-CD45 AF700 (Biolegend), anti-CD11b-FITC (Biolegend), anti-CD11c-PE Cy-7 (BD), anti-Siglec-F- BV711 (BD), anti-CD64-BV605 (Biolegend), anti-CD24-PE (Biolegend), anti-Ly-6G-PerCP-Cy5.5 (Biolegend), anti-CD103-BV510 (Biolegend), anti-CD86-APC (Biolegend), anti-Ly6C (PE dazzle 594) and anti-MHC II BV421 (Biolegend) for 30 min at 4 °C. Total 10^6 gated events per sample were collected using Fortessa flow cytometer (Becton Dickinson, San Diego, CA), and results were analyzed using FlowJo 10.4.2 software.

Quantitation of MAIT cytokine transcripts by real-time PCR

MAIT cells ($CD3^+$ $CD44^+$ $TCR\beta^+$ MR1-5-OP-RU $tetramer^+$) and non-MAIT (MR1-5-OP-RU $tetramer^-$ $TCR\beta^+$) $CD3^+$ T cell populations were sorted into 350 µl RLT plus buffer from the Qiagen Allprep DNA/RNA micro kit. Nucleic acid extraction was performed according to manufacturer's instructions (Qiagen Allprep RNA/DNA). cDNA was synthesized using SuperScript VILO cDNA Synthesis Kit and qRT-PCR analysis on *Ifng, Il17a, Gzmb* and *Prf1* genes was performed with specific TaqMan primers and TaqMan Fast Advanced Master Mix (Applied Biosystems). The mRNA levels of specific genes were determined by the relative standard curve method, normalized against housekeeping ribosomal protein L32 levels. ΔCT was calculated as CT_{gene} – $CT_{housekeeping}$ and ΔΔCT was calculated as $\Delta CT_{CLP} - \Delta CT_{sham.}$

Mouse cytokines

Following lung dissociation, cells were passed through a 70-µm nylon mesh. Cells and debris were removed from the suspension via centrifugation at 300 x g for 10 min and supernatant were collected and stored at -80°C for later use. Lung cytokine levels were assessed from the supernatant samples via LEGENDplex (mouse inflammation panel 13-plex; BioLegend) kit per manufacturer's instructions. Serum samples were 2-fold diluted and cytokine levels were assessed using same kit as per manufacturer's instructions. Cytokine levels were acquired using a FACSCanto II flow cytometer (BD Biosciences, San Jose, CA), and analyses were performed using LEGENDplex data analysis software (BioLegend).

Ex vivo co-culture of lung Ly6C$^+$ CD11b$^+$ monocytes with MAITs

Lung MAITs were expanded *ex vivo* using a previously published method for expansion of human MAIT cells (27). Briefly, lung homogenates from healthy WT mice were cultured for 14 days in presence of mouse recombinant IL-2 and sulfate latex beads of 5-OP-RU/MR1 artificial antigen-presenting cells. To isolate monocytes, lung cells from healthy WT mice were surface stained with anti-CD45 AF700 (Biolegend), anti-CD11b-FITC (Biolegend), anti-Siglec-F- BV711 (BD), and anti- Ly6C (PE dazzle 594) for 30 min at 4 °C. We obtained CD45$^+$ Siglec-F$^-$ Ly6C$^+$ CD11b$^+$ monocytes by flow sorting on a FACS Aria II (BD, Franklin Lakes, NJ, USA). We incubated 20,000 MAITs with 10,000 monocytes for 18 hours, in a total volume of 200µl in a 96-well U-bottom plates. MAIT-monocyte co-culture was stimulated with 200nM 5-A-RU and 50µM MeG (28) in RPMI 1640 with 10% FBS with 1% penicillin/streptomycin and 1% HEPES. MAIT cells that were stimulated/unstimulated and monocytes that were stimulated/unstimulated were

kept as controls. After 18 hours, cell supernatant was collected and stored at -20°C. We measured IFN-γ and GM-CSF levels in supernatants using ELISA as per manufacturer's instruction in Biolegend ELISA MAX™ standard sets for mouse IFN-γ and for mouse GM-CSF.

Human Subjects

Patients admitted to an academic medical intensive care unit (ICU) with a primary diagnosis of severe sepsis or septic shock were prospectively enrolled within 48 (±24) hours of ICU admission. Sepsis was defined using the consensus criteria (40, 41) at the time this study was actively recruiting, defined as suspected or confirmed systemic infection and organ dysfunction as defined by a sequential organ failure assessment (SOFA) score ≥2 above baseline. Septic shock was defined as sepsis and an elevated lactate > 2mmol/L or the need for vasopressors. Blood samples were collected from septic patients upon study enrollment (Day 1, after ICU admission for sepsis) and again in the same subjects ~90 days after enrollment (Day 90). Venous blood was collected and centrifuged over a Ficoll-Hypaque density gradient using the standard protocol to isolate peripheral blood mononuclear cells (PBMCs), which were either cryopreserved or used directly. Samples from healthy donors were collected and processed following the same procedure.

Analysis of MAIT cytokine expression by flow cytometry.

For phenotypic analysis of MAIT cells, PBMCs were thawed from -80ºC and were stained for surface markers: anti-CD137-Alexa Fluor 700 (Biolegend), anti-CD3-

BUV395 (BD biosciences), anti-CD8-PE-Cy5.5 (Molecular Probes), anti-CD4-BUV496 (BD Biosciences), anti-Vα7.2-BV711 (Biolegend), anti-LAG3-BV785 (Biolegend), anti-CD25-BV650 (Biolegend), anti-PD-1-BV605 (Biolegend), anti-CD161-BV510 (Biolegend), anti-CD69-PE-Cy5 (Biolegend), anti-HLA-DR-FITC (Biolegend), anti-TIM3-BV421 (Biolegend), anti-CD38-PE-Cy7 (Biolegend), and anti-human MR1 5-OP-RU Tetramer (NIH Tetramer Core Facility). PBMCs that were cultured and stimulated with 1100-2 *E. coli* (*E. coli* Genetic Stock Center (CGSC),Yale University) at multiplicity of infection (MOI) of 10 for 18 hours were stained for surface markers: anti-human MR1 5-OP-RU Tetramer (NIH Tetramer Core Facility), anti-CD3-BUV395 (BD biosciences), anti-CD8-PE-Cy5.5 (Molecular Probes), anti-CD4-BUV496 (BD Biosciences), anti-Vα7.2-BV711 (Biolegend), anti-LAG3-BV785 (Biolegend), anti-CD25-BV650 (Biolegend), anti-PD-1-BV605 (Biolegend), anti-CD161-BV510 (Biolegend), anti-CD69-PE-Cy5 (Biolegend) and intracellularly stained for: anti-IL-17A-FITC (Biolegend), anti-IFN-γ-PE-Cy7 (Biolegend), anti-TNFα-ef450 (Molecular Probes), anti-Granzyme B-Alexa Fluor 700 (Biolegend). All samples were acquired using a 5-laser BD LSRFortessa II flow cytometer (BD Biosciences) and analyzed using FlowJo software v10 (Tree Star, Inc. Ashland, Oreg). Unstimulated controls were used to define positive population.

Statistics and power calculations

Comparisons between independent groups were performed with unpaired t test. The Mann-Whitney *U* test was used for comparison of continuous variables between two groups and results of lung cytokine analysis were presented as mean ± standard

deviation. For comparisons of more than two groups, one-way ANOVA with Tukey's multiple comparison test was used.

For comparisons of healthy subjects with day 1 or day 90 septic patients Mann-Whitney *U* test was used and for comparisons of paired day 1 and day 90 samples Wilcoxon test was used. GraphPad Prism 8.3.0 software was used for all statistical analysis and $p < 0.05$ was considered statistically significant.

We used Cox proportional-hazards (coxph) model with non-bedding-transferred mice as reference for determining power calculation for the number of mice needed in the bedding transfer experiment. Formula used was: coxph(formula = Surv(t, event) ~ group, data = exp) with coef = 2.1525, exp(coef) = 8.6065, se(coef) = 0.7724, z = 2.787 and p group = 0.00532. Likelihood ratio test = 11.35 on 1 df, p=0.0007563, n= 30, number of events= 13. In order to observe the hazard ratio from this study (8.6065) with 80% power and type I error 0.05, we need to observe 7 deaths. In order to determine sample size, we divided 7 by the expected rate of death overall. For an expected death rate of 50%, we needed a sample size of 14; for an expected death rate of 25%, we needed a sample size of 28.

Study approval: Each patient or a legally authorized representative provided written, informed consent. The institutional review board approved this study. All animals were maintained and experiments were performed in accordance with The University of Utah

and Institutional Animal Care and Use Committee (IACUC) approved guidelines (protocol # 18-10012).

Acknowledgements: This research was supported by the National Institutes of Health (AI130378 to D.T.L., HL092161, AG040631, and AG048022 to M.T.R., TL1TR002540 to D.L., T32 HG008962 to C.P.A.], and a University of Utah 3i Initiative Seed Grant (to D.T.L, M.T.R., J.S.H.). We would like to thank all the study subjects who participated in the study. We thank Kelin Li and Jeffrey Aube for providing 5-amino-6-D-ribitylaminouracil (5-A-RU) for our study. We would like to thank Michael C Graves and Alexandra Heitkamp for help in laboratory and Ben Brintz, Study Design and Biostatistics Center, University of Utah, for help with statistics and power calculations. We would also like to thank the staff of the University of Utah Flow Cytometry Core and the Office of Comparative Medicine.

Figure Legends

Figure 1. Sepsis induces MAIT-specific changes in inflammatory cytokine expression. (A) Gating strategy for isolation of MAIT cells. In first plot, lymphocytes with $CD45R^-$ B cells were excluded by electronic gating and $CD44^+$ $CD3^+$ T cells were gated to define MAIT cells as $TCR\beta^+$ MR1-5OP-RU-$tetramer^+$ cells. (B) Percentage of $TCR\beta^+$ MR1-$tetramer^+$ MAIT cells, of $CD3^+$ T cells in WT mice after 18 hours of CLP or sham operation. (C) Gene expression in MAIT cells isolated using flow cytometric

sorting of homogenized lung tissue after CLP or sham operation (n = 5 per group), as determined by qRT-PCR for *Ifng, Il17a* and *GzmB* genes, (D) *Ifng, Il17a,* and *GzmB* mRNA expression in non-MAIT (MR1-tetramer^{-} TCRβ^{+}) CD3^{+} T cell populations. Data are expressed as mean ± SD, and unpaired *t*-test was used for comparisons (data passed Shapiro-Wilk normality test).

Figure 2. Sepsis induces lower IFNγ production in MAIT cells. (**A**) Percentage frequencies of IFNγ expression in MAIT cells of lung tissue, 18 hours after CLP or sham operation (n = 7 per group), as determined by intracellular cytokine staining and flow cytometry. (**B**) MFI of IFNγ staining in MAIT cells. (**C**) Percentage frequencies of IFNγ expression in NON MAIT cells of lung tissue. **(D and E)** Percentage frequencies of IFNγ expression in *i*NKT and TCRγδ cells. Data are expressed as mean ± SD, and unpaired *t*-test was used for comparisons (data passed Shapiro-Wilk normality test).

Figure 3. *Mr1*$^{-/-}$ mice had higher sepsis-induced mortality and bacterial burden compared to wildtype mice. (**A**) Age matched *Mr1*$^{-/-}$ and WT mice (n = 15 per group) underwent CLP to induce polymicrobial sepsis. Survival was recorded over a period of 4-5 days (WT versus *Mr1*$^{-/-}$ mice, *** p = 0.0007). Data represents two independent experiments. Statistical analysis was performed using Log-rank (Mantel-Cox) test. (**B**) Blood was collected from WT and *Mr1*$^{-/-}$ mice (n = 8-10 per group) 18 h post CLP, and serial dilutions were plated on Luria Broth (LB) agar plates. Colony-forming units (CFU) were determined 24 h after plating and were expressed as CFU/ml. Statistical analysis was performed using Mann-Whitney test. **(C)** Bedding transfer procedure (detailed in

methods section) was used to exchange gut microbiome between age matched *Mr1*$^{-/-}$ and WT mice (total n = 31 for *Mr1*$^{-/-}$ mice and total n = 30 for WT mice) before inducing sepsis by CLP. Survival was recorded over a period of 4-5 days (WT versus *Mr1*$^{-/-}$ mice, * p = 0.03). Data represents three independent experiments. Statistical analysis was performed using Log-rank (Mantel-Cox) test.

Figure 4. *Mr1*$^{-/-}$ mice had significantly lower levels of cytokines in lung tissue at 18 h post CLP. Levels of (**A**) IFN-γ, (**B**) IL-17A, (**C**) TNF-α, (**D**) IL-10, and (**E**) GM-CSF were assessed in lungs isolated from WT and *Mr1*$^{-/-}$ mice at 18 h post CLP or sham operation, using a bead-based immunoassay kit. Bars represent mean cytokine levels ± SD. The graphs represent two independent experiments (WT n= 8, *Mr1*$^{-/-}$ n = 7). The statistical significance was determined by the nonparametric Mann–Whitney test.

Figure 5. Lower frequencies of interstitial macrophages and monocytic dendritic cells in lungs of *Mr1*$^{-/-}$ mice at 18 h post CLP. Lung cells were obtained from WT (n=5) and *Mr1*$^{-/-}$ mice (n = 5-6) at 18 h post CLP or sham operation, stained for surface markers and analyzed using flow cytometry. Percentage frequencies of (**A**) interstitial macrophages, (**B**) monocytic dendritic cells, (**C**) alveolar macrophages and (**D**) plasmacytoid dendritic cells and (**E**) neutrophils were compared between the groups by nonparametric Mann–Whitney test. Data were expressed as mean ± SD of two independent experiments.

Figure 6. Altered frequency and phenotype of human MAIT cells in sepsis compared to healthy donors (HD). (**A**) Gating strategy for isolation of MAIT cells from PBMCs. (**B**) Percentage of MR1-tetramer^{+} MAIT cells in CD3^{+} T cells, (**C**) Representative flow plots and percentage of MAIT cells in paired Day 1 and Day 90 septic patients (n = 12 per group), (**D**) Representative flow plots and surface expression of activation markers as percentage of MAIT cells, (**E**) Surface expression of inhibitory receptors, as percentage of MAIT cells. Data were expressed as mean ± SD of two independent experiments. Mann-Whitney test was used to compare HD with septic patients and Wilcoxon test was used for comparisons of paired D1 and D90 samples. ***P < 0.001, **P < 0.01, *P < 0.05. NS, P > 0.05.

Figure 7. Lower frequencies of IFNγ^{+} MAIT cells in day 1 septic patients compared to HD and day 90 paired septic patients. PBMCs obtained from septic patients and healthy donors (n = 12 per group) were stimulated with *E.coli* at moi of 10 and intracellular expression of (**A**) IFN-γ, (**B**) IL-17, (**C**) TNF-α and (**D**) granzyme B by MAIT cells were analyzed using flow cytometry (open circle shows unstimulated and closed circle shows stimulated data). Data were expressed as mean ± SD of two independent experiments. Mann-Whitney test was used for comparisons of HD with septic patients and Wilcoxon test was used for comparisons of paired D1 and D90 samples. ***P < 0.001, **P < 0.01, *P < 0.05. NS, P > 0.05.

Supplementary Figure Legends

Figure 3 – figure supplement 1. *Mr1*$^{-/-}$ mice had significantly higher mortality from ExPEC sepsis, compared to WT mice. Graph shows survival curves after intraperitoneal injection with 1x10^{6} cfu of Extraintestinal pathogenic Escherichia coli (ExPEC) F11 strain. Statistical analysis was performed using Log-rank (Mantel-Cox) test.

Figure 4-figure supplement 1. *Mr1*$^{-/-}$ mice had reduced IFNγ and TNFα but similar levels of other cytokines in serum at 18 h post CLP. Levels of (A) IFN-γ, (B) IL-17A, (C) TNF-α, (D) IL-10, and (E) GM-CSF were assessed in serum of WT and *Mr1*$^{-/-}$ mice at 18 h post CLP using a bead-based immunoassay kit. Bar represent mean cytokine level ± SD. The graphs represents average of two independent experiment (WT n = 7-8, *Mr1*$^{-/-}$ n = 6-7). The statistical significance was determined by the nonparametric Mann–Whitney test.

Figure 4-figure supplement 2. *Mr1*$^{-/-}$ mice had reduced IL-10 but similar levels of other cytokines in liver at 18 h post CLP. Levels of (A) IFN-γ, (B) IL-17A, (C) TNF-α, (D) IL-10, and (E) GM-CSF were assessed in liver of WT and *Mr1*$^{-/-}$ mice at 18 h post CLP using a bead-based immunoassay kit. Bar represent mean cytokine level ± SD. The graphs represents one experiment (WT n = 5, *Mr1*$^{-/-}$ n = 4). The statistical significance was determined by the nonparametric Mann–Whitney test.

Figure 4-figure supplement 3. *Mr1*$^{-/-}$ mice had similar levels of other cytokines in gut at 18 h post CLP. Levels of (A) IFN-γ, (B) IL-17A, (C) TNF-α, (D) IL-10, and (E) GM-CSF were assessed in gut of WT and *Mr1*$^{-/-}$ mice at 18 h post CLP using a bead-based immunoassay kit. Bar represent mean cytokine level ± SD. The graphs represents one experiment (WT n = 5, *Mr1*$^{-/-}$ n = 4). The statistical significance was determined by the nonparametric Mann–Whitney test.

Figure 5-figure supplement 1. Higher amounts of IFN-γ and GM-CSF production in *ex-vivo* stimulated MAIT-monocytes coculture. *Ex-vivo* expanded lung MAITs were cultured with Ly6C^{+} CD11b^{+} monocytes isolated from lungs of WT mice for 18 hours. Levels of (A) IFN-γ and (B) GM-CSF in supernatants were measured using Biolegend ELISA MAX™ standard sets for mouse IFN-γ and for mouse GM-CSF. Data shown are mean ± SD, and statistical significance was determined by using unpaired *t*-test (data passed Shapiro-Wilk normality test).

Figure 5-figure supplement 2. Frequencies of other unconventional T cells such as invariant natural killer T cells (*i*NKT) and γδ T cells post CLP. Lung cells were obtained from WT and and *Mr1*$^{-/-}$ mice at 18 h post CLP or sham operation, stained for surface markers and analyzed using flow cytometry. Percentage frequencies of (A) *i*NKT cells and (B) γδ T cells were compared between the groups using one-way ANOVA with Tukey's multiple comparison test.

References

1. Singer M, Deutschman CS, Seymour CW, Shankar-Hari M, Annane D, Bauer M, et al. The Third International Consensus Definitions for Sepsis and Septic Shock (Sepsis-3). *JAMA.* 2016;315(8):801-10.
2. Fleischmann C, Scherag A, Adhikari NK, Hartog CS, Tsaganos T, Schlattmann P, et al. Assessment of Global Incidence and Mortality of Hospital-treated Sepsis. Current Estimates and Limitations. *Am J Respir Crit Care Med.* 2016;193(3):259-72.
3. Gentile LF, Cuenca AG, Efron PA, Ang D, Bihorac A, McKinley BA, et al. Persistent inflammation and immunosuppression: a common syndrome and new horizon for surgical intensive care. *J Trauma Acute Care Surg.* 2012;72(6):1491-501.
4. Otto GP, Sossdorf M, Claus RA, Rodel J, Menge K, Reinhart K, et al. The late phase of sepsis is characterized by an increased microbiological burden and death rate. *Crit Care.* 2011;15(4):R183.
5. Hotchkiss RS, Monneret G, and Payen D. Immunosuppression in sepsis: a novel understanding of the disorder and a new therapeutic approach. *Lancet Infect Dis.* 2013;13(3):260-8.
6. Cohen J, Opal S, and Calandra T. Sepsis studies need new direction. *Lancet Infect Dis.* 2012;12(7):503-5.
7. Ranieri VM, Thompson BT, Barie PS, Dhainaut JF, Douglas IS, Finfer S, et al. Drotrecogin alfa (activated) in adults with septic shock. *N Engl J Med.* 2012;366(22):2055-64.
8. Williams SC. After Xigris, researchers look to new targets to combat sepsis. *Nat Med.* 2012;18(7):1001.
9. Hotchkiss RS, Moldawer LL, Opal SM, Reinhart K, Turnbull IR, and Vincent J-L. Sepsis and septic shock. *Nature Reviews Disease Primers.* 2016;2(1):16045.
10. Porcelli S, Yockey CE, Brenner MB, and Balk SP. Analysis of T cell antigen receptor (TCR) expression by human peripheral blood CD4-8- alpha/beta T cells demonstrates preferential use of several V beta genes and an invariant TCR alpha chain. *J Exp Med.* 1993;178(1):1-16.
11. Lee OJ, Cho Y-N, Kee S-J, Kim M-J, Jin H-M, Lee S-J, et al. Circulating mucosal-associated invariant T cell levels and their cytokine levels in healthy adults. *Experimental Gerontology.* 2014;49:47-54.
12. Martin E, Treiner E, Duban L, Guerri L, Laude H, Toly C, et al. Stepwise Development of MAIT Cells in Mouse and Human. *PLoS Biology.* 2009;7(3):e1000054.
13. Georgel P, Radosavljevic M, Macquin C, and Bahram S. The non-conventional MHC class I MR1 molecule controls infection by Klebsiella pneumoniae in mice. *Mol Immunol.* 2011;48(5):769-75.
14. Chua W-J, Truscott SM, Eickhoff CS, Blazevic A, Hoft DF, and Hansen TH. Polyclonal mucosa-associated invariant T cells have unique innate functions in bacterial infection. *Infection and immunity.* 2012;80(9):3256-67.
15. Le Bourhis L, Martin E, Peguillet I, Guihot A, Froux N, Core M, et al. Antimicrobial activity of mucosal-associated invariant T cells. *Nat Immunol.* 2010;11(8):701-8.
16. Grimaldi D, Le Bourhis L, Sauneuf B, Dechartres A, Rousseau C, Ouaaz F, et al. Specific MAIT cell behaviour among innate-like T lymphocytes in critically ill patients with severe infections. *Intensive Care Med.* 2014;40(2):192-201.
17. Fein AM, Lippmann M, Holtzman H, Eliraz A, and Goldberg SK. The risk factors, incidence, and prognosis of ARDS following septicemia. *Chest.* 1983;83(1):40-2.
18. Martin GS, Mannino DM, Eaton S, and Moss M. The epidemiology of sepsis in the United States from 1979 through 2000. *N Engl J Med.* 2003;348(16):1546-54.

19. Rahimpour A, Koay HF, Enders A, Clanchy R, Eckle SBG, Meehan B, et al. Identification of phenotypically and functionally heterogeneous mouse mucosal-associated invariant T cells using MR1 tetramers. *The Journal of Experimental Medicine.* 2015;212(7):1095-108.
20. Yost CC, Schwertz H, Cody MJ, Wallace JA, Campbell RA, Vieira-de-Abreu A, et al. Neonatal NET-inhibitory factor and related peptides inhibit neutrophil extracellular trap formation. *J Clin Invest.* 2016;126(10):3783-98.
21. Middleton EA, Rowley JW, Campbell RA, Grissom CK, Brown SM, Beesley SJ, et al. Sepsis alters the transcriptional and translational landscape of human and murine platelets. *Blood.* 2019;134(12):911-23.
22. Smith AD, Foss ED, Zhang I, Hastie JL, Giordano NP, Gasparyan L, et al. Microbiota of MR1 deficient mice confer resistance against Clostridium difficile infection. *PLOS ONE.* 2019;14(9):e0223025.
23. Miyoshi J, Leone V, Nobutani K, Musch MW, Martinez-Guryn K, Wang Y, et al. Minimizing confounders and increasing data quality in murine models for studies of the gut microbiome. *PeerJ.* 2018;6:e5166-e.
24. Xiao X, and Cai J. Mucosal-Associated Invariant T Cells: New Insights into Antigen Recognition and Activation. *Frontiers in Immunology.* 2017;8(1540).
25. Hegde P, Weiss E, Paradis V, Wan J, Mabire M, Sukriti S, et al. Mucosal-associated invariant T cells are a profibrogenic immune cell population in the liver. *Nature Communications.* 2018;9(1):2146.
26. Meierovics AI, and Cowley SC. MAIT cells promote inflammatory monocyte differentiation into dendritic cells during pulmonary intracellular infection. *J Exp Med.* 2016;213(12):2793-809.
27. Liu Y, Wang W, Wu X, and Weng X. In: Liu C ed. *T-Cell Receptor Signaling: Methods and Protocols*. New York, NY: Springer US; 2020:285-93.
28. Li K, Vorkas CK, Chaudhry A, Bell DL, Willis RA, Rudensky A, et al. Synthesis, stabilization, and characterization of the MR1 ligand precursor 5-amino-6-D-ribitylaminouracil (5-A-RU). *PLOS ONE.* 2018;13(2):e0191837.
29. Hu CK, Venet F, Heffernan DS, Wang YL, Horner B, Huang X, et al. The role of hepatic invariant NKT cells in systemic/local inflammation and mortality during polymicrobial septic shock. *J Immunol.* 2009;182(4):2467-75.
30. Heffernan DS, Monaghan SF, Thakkar RK, Tran ML, Chung C-S, Gregory SH, et al. Inflammatory Mechanisms in Sepsis: Elevated Invariant Natural Killer T-Cell Numbers in Mouse and Their Modulatory Effect on Macrophage Function. *Shock.* 2013;40(2):122-8.
31. Andreu-Ballester JC, Tormo-Calandin C, Garcia-Ballesteros C, Perez-Griera J, Amigo V, Almela-Quilis A, et al. Association of γδ T cells with disease severity and mortality in septic patients. *Clinical & vaccine immunology.* 2013;20(5):738-46.
32. Hirsh M, Dyugovskaya L, Kaplan V, and Krausz MM. Response of lung gammadelta T cells to experimental sepsis in mice. *Immunology.* 2004;112(1):153-60.
33. Bennett MS, Trivedi S, Iyer AS, Hale JS, and Leung DT. Human mucosal-associated invariant T (MAIT) cells possess capacity for B cell help. *J Leukoc Biol.* 2017;102(5):1261-9.
34. Le Bourhis L, Martin E, Péguillet I, Guihot A, Froux N, Coré M, et al. Antimicrobial activity of mucosal-associated invariant T cells. *Nature Immunology.* 2010;11(8):701-8.
35. Ghazarian L, Caillat-Zucman S, and Houdouin V. Mucosal-Associated Invariant T Cell Interactions with Commensal and Pathogenic Bacteria: Potential Role in Antimicrobial Immunity in the Child. *Frontiers in Immunology.* 2017;8(1837).
36. Leeansyah E, Ganesh A, Quigley MF, Sonnerborg A, Andersson J, Hunt PW, et al. Activation, exhaustion, and persistent decline of the antimicrobial MR1-restricted MAIT-cell population in chronic HIV-1 infection. *Blood.* 2013;121(7):1124-35.

37. Shaler CR, Choi J, Rudak PT, Memarnejadian A, Szabo PA, Tun-Abraham ME, et al. MAIT cells launch a rapid, robust and distinct hyperinflammatory response to bacterial superantigens and quickly acquire an anergic phenotype that impedes their cognate antimicrobial function: Defining a novel mechanism of superantigen-induced immunopatho. *PLOS Biology.* 2017;15(6):e2001930.
38. Leung DT, Bhuiyan TR, Nishat NS, Hoq MR, Aktar A, Rahman MA, et al. Circulating mucosal associated invariant T cells are activated in Vibrio cholerae O1 infection and associated with lipopolysaccharide antibody responses. *PLoS Negl Trop Dis.* 2014;8(8):e3076.
39. Smith JL, Fratamico PM, and Gunther NW. Extraintestinal pathogenic Escherichia coli. *Foodborne Pathog Dis.* 2007;4(2):134-63.
40. Bone RC, Balk RA, Cerra FB, Dellinger RP, Fein AM, Knaus WA, et al. Definitions for sepsis and organ failure and guidelines for the use of innovative therapies in sepsis. The ACCP/SCCM Consensus Conference Committee. American College of Chest Physicians/Society of Critical Care Medicine. *Chest.* 1992;101(6):1644-55.
41. American College of Chest Physicians/Society of Critical Care Medicine Consensus Conference: definitions for sepsis and organ failure and guidelines for the use of innovative therapies in sepsis. *Crit Care Med.* 1992;20(6):864-74.

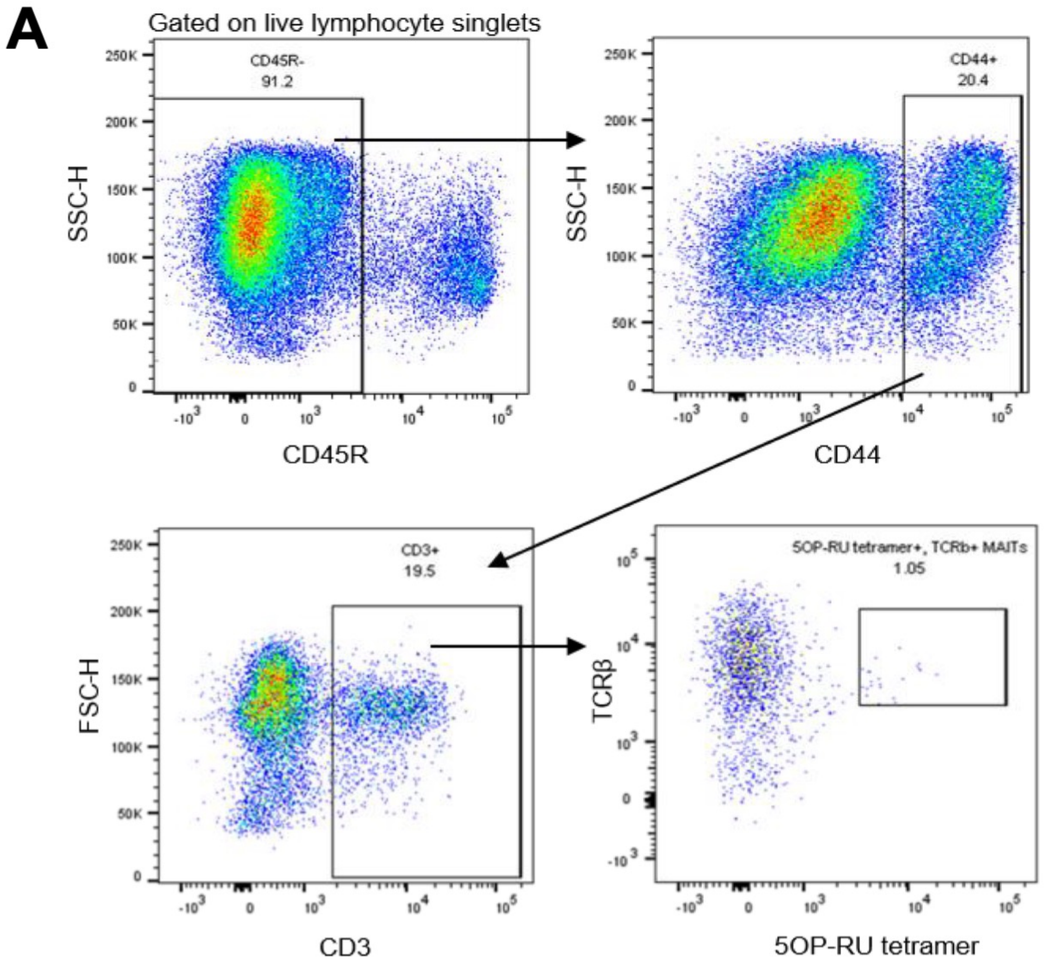
A
Gated on live lymphocyte singlets
CD45R-
91.2
SSC-H
CD45R
CD44+
20.4
SSC-H
CD44
CD3+
19.5
FSC-H
CD3
5OP-RU tetramer+, TCRb+ MAITs
1.05
TCRβ
5OP-RU tetramer

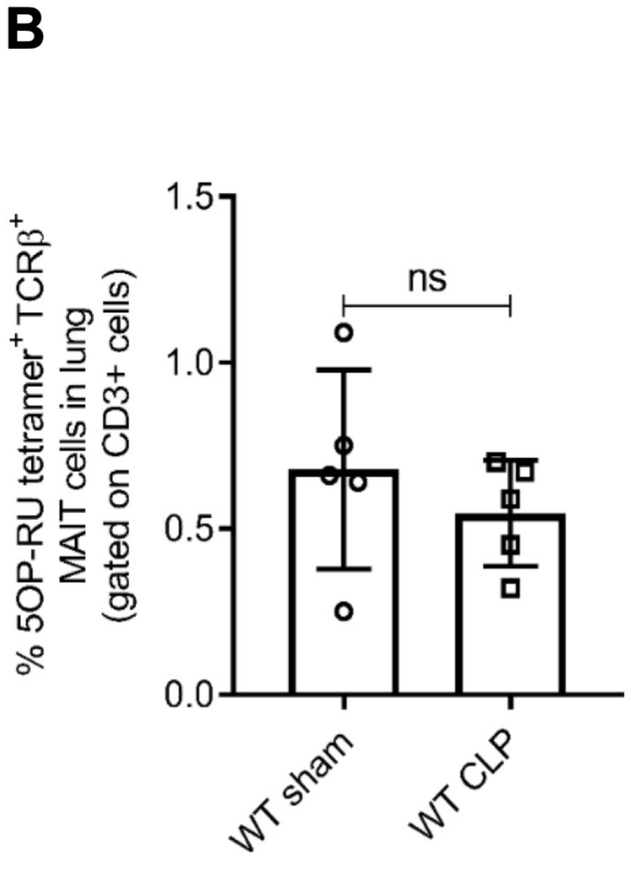
B
% 5OP-RU tetramer+ TCRβ+
MAIT cells in lung
(gated on CD3+ cells)
ns
WT sham
WT CLP

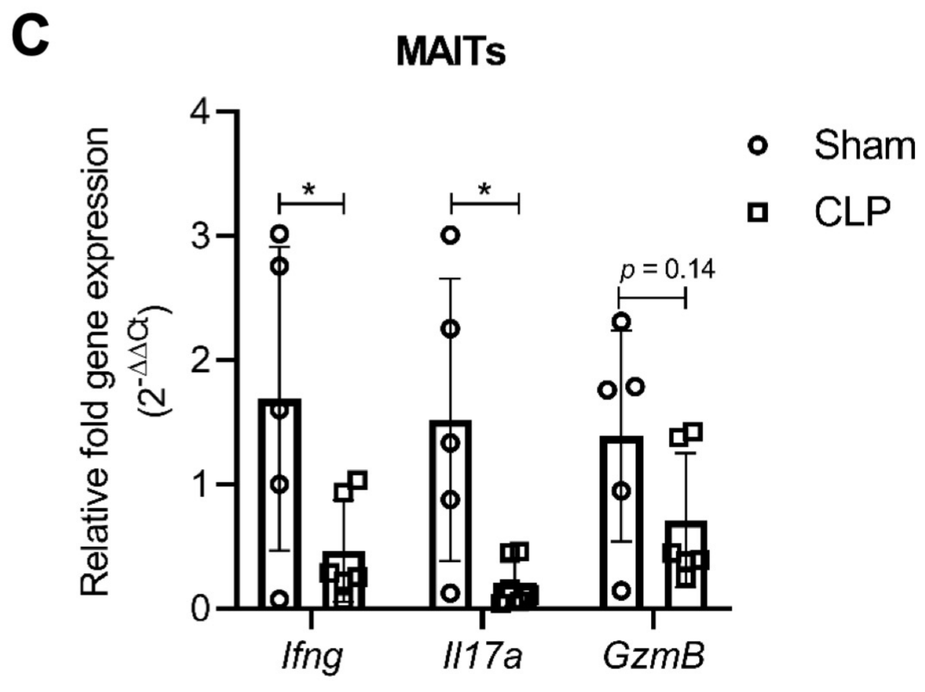
C
MAITs
Relative fold gene expression
(2-ΔΔCt)
Sham
CLP
*
*
p = 0.14
Ifng
Il17a
GzmB

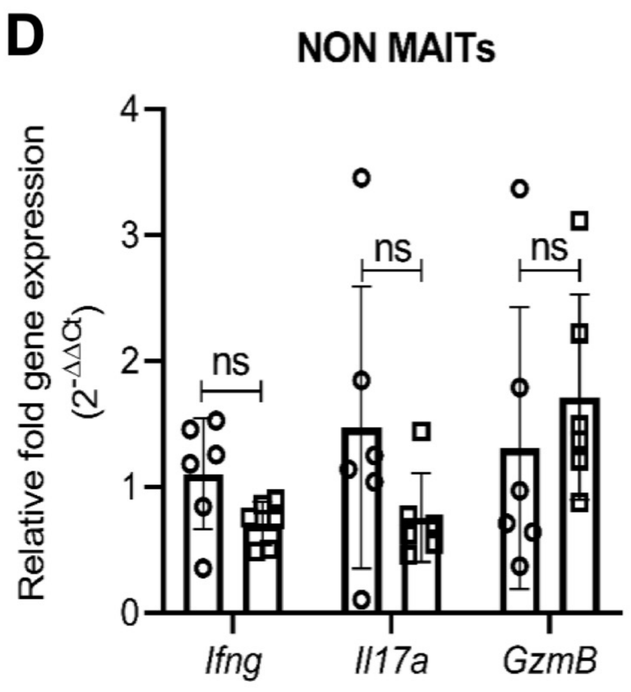
D
NON MAITs
Relative fold gene expression
(2-ΔΔCt)
ns
ns
ns
Ifng
Il17a
GzmB

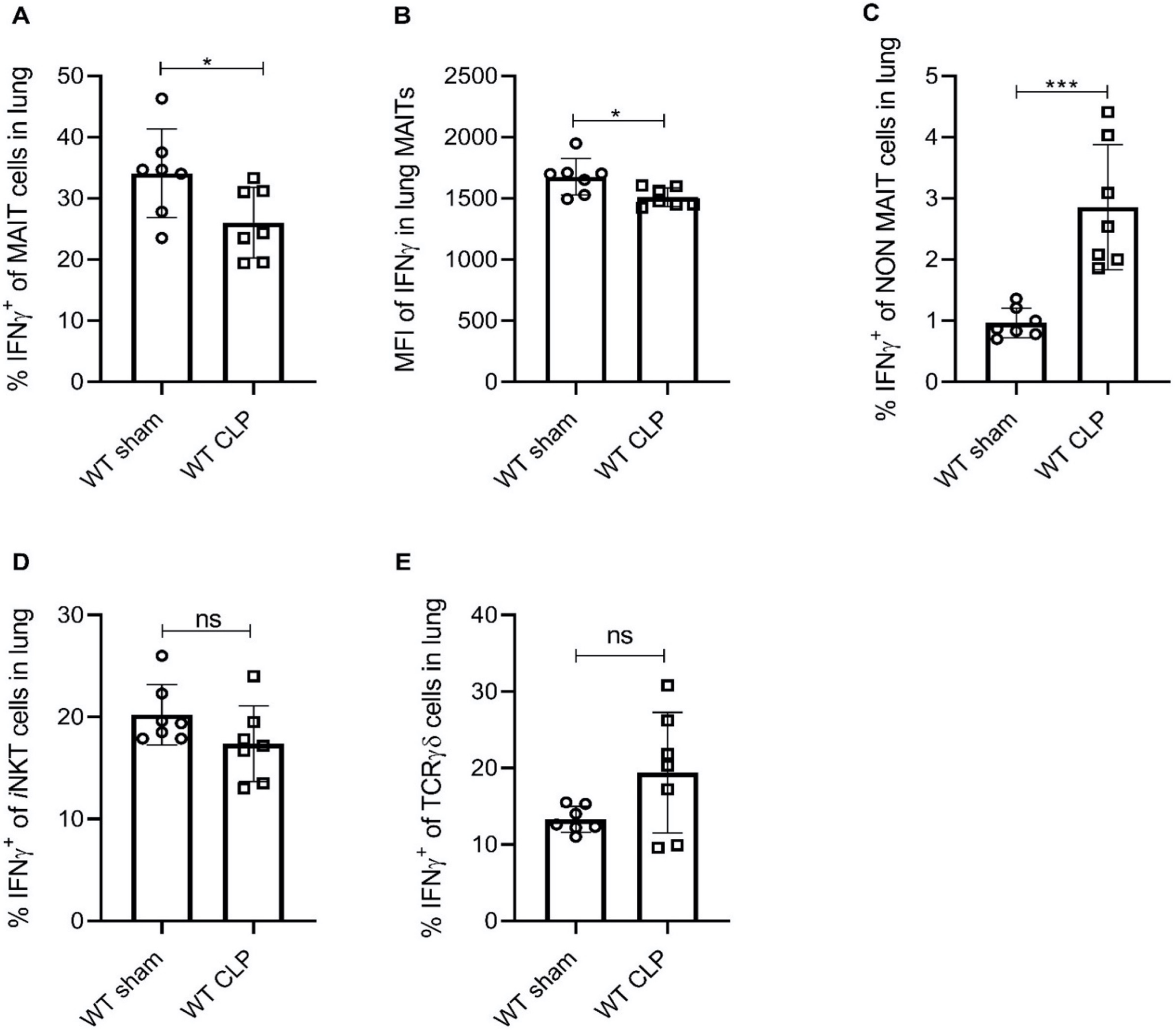
A
% IFNγ+ of MAIT cells in lung
50
40
30
20
10
0
*
WT sham
WT CLP
B
MFI of IFNγ in lung MAITs
2500
2000
1500
1000
500
0
*
WT sham
WT CLP
C
% IFNγ+ of NON MAIT cells in lung
5
4
3
2
1
0
***
WT sham
WT CLP
D
% IFNγ+ of iNKT cells in lung
30
20
10
0
ns
WT sham
WT CLP
E
% IFNγ+ of TCRγδ cells in lung
40
30
20
10
0
ns
WT sham
WT CLP

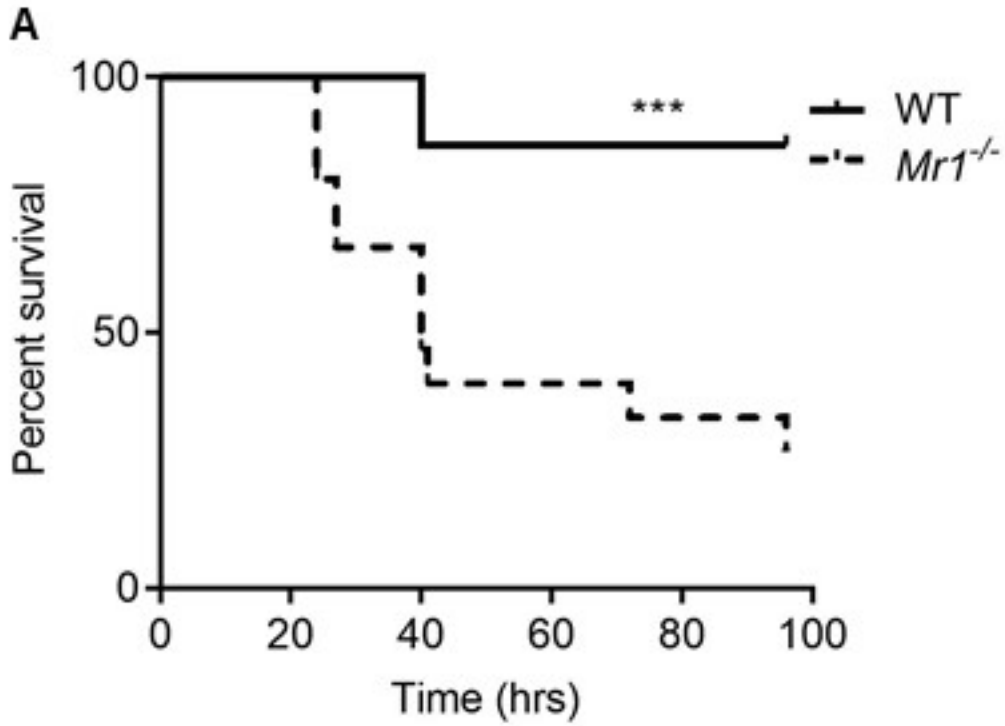
A
100
50
0
Percent survival
0
20
40
60
80
100
Time (hrs)
***
WT
Mr1-/-

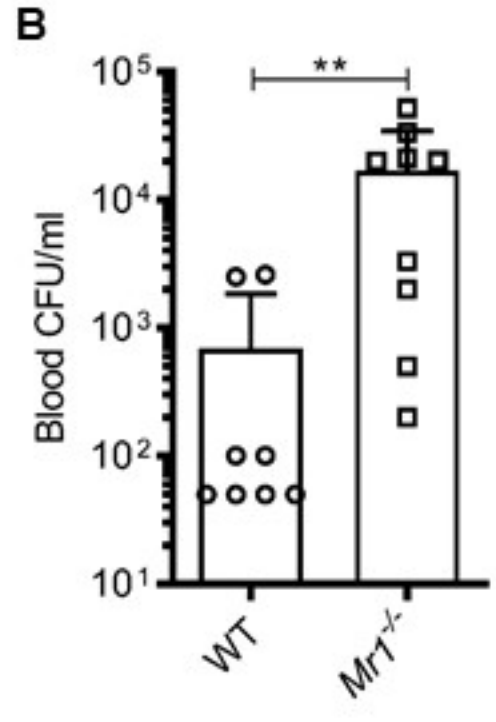
B
10^5
10^4
10^3
10^2
10^1
Blood CFU/ml
**
WT
Mr1-/-

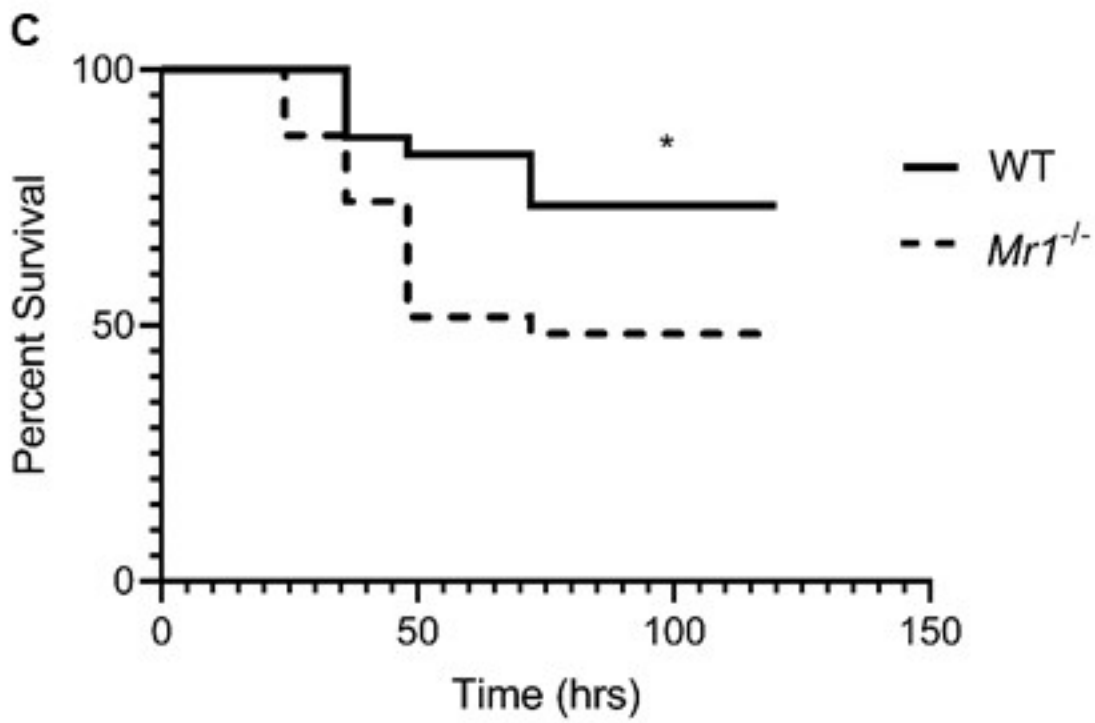
C
100
50
0
Percent Survival
0
50
100
150
Time (hrs)
*
WT
Mr1-/-

A

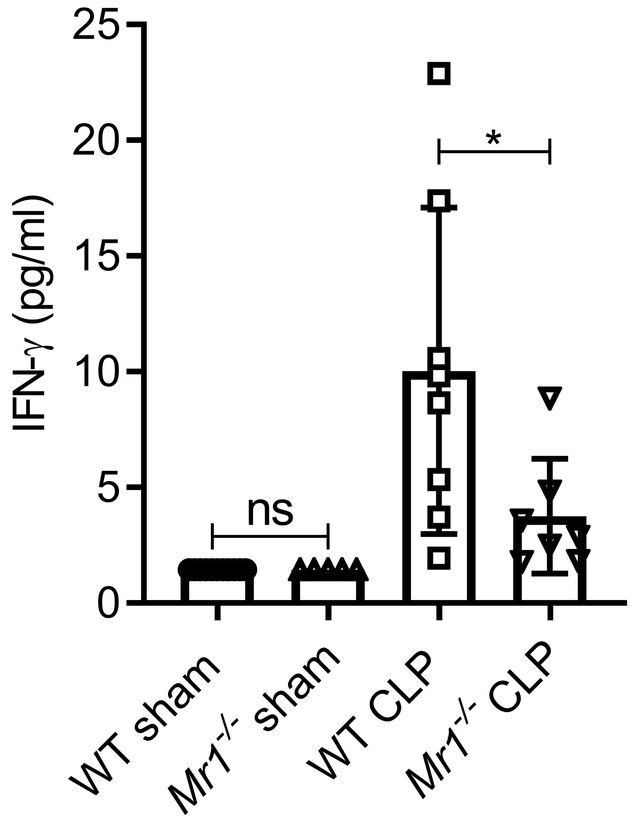
IFN-γ (pg/ml)
25
20
15
10
5
0
ns
*
WT sham
Mr1-/- sham
WT CLP
Mr1-/- CLP

B

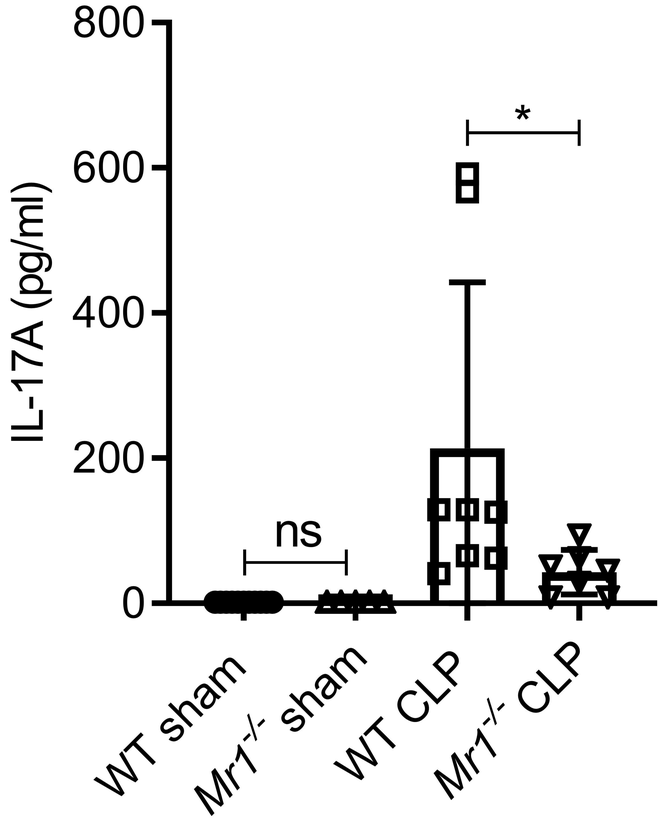
IL-17A (pg/ml)
800
600
400
200
0
ns
*
WT sham
Mr1-/- sham
WT CLP
Mr1-/- CLP

C

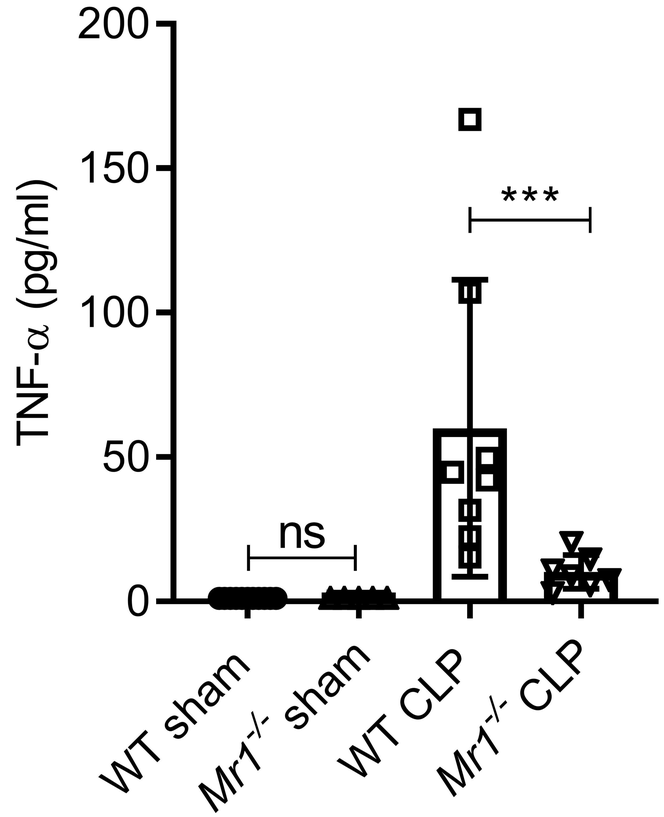
TNF-α (pg/ml)
200
150
100
50
0
ns
***
WT sham
Mr1-/- sham
WT CLP
Mr1-/- CLP

D

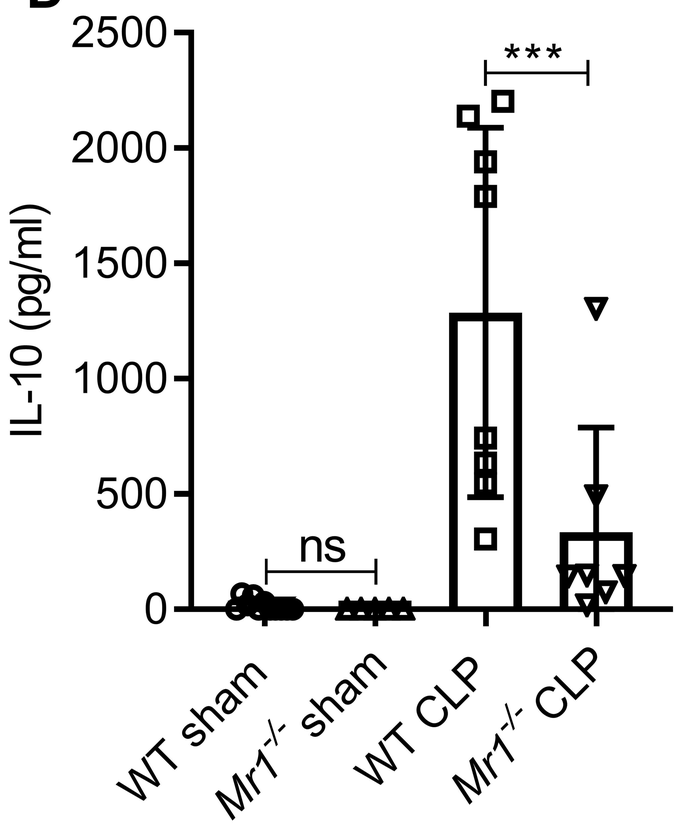
IL-10 (pg/ml)
2500
2000
1500
1000
500
0
ns
***
WT sham
Mr1-/- sham
WT CLP
Mr1-/- CLP

E

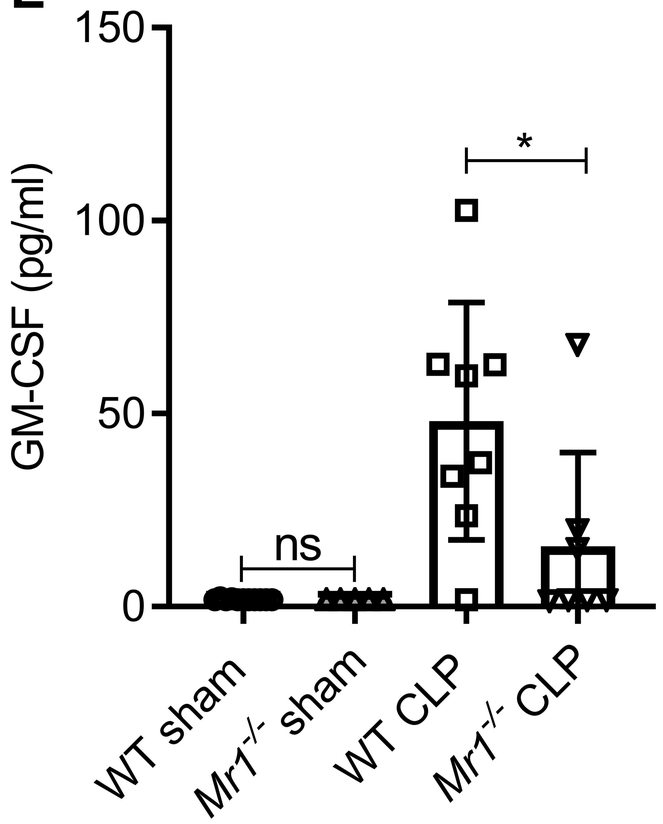
GM-CSF (pg/ml)
150
100
50
0
ns
*
WT sham
Mr1-/- sham
WT CLP
Mr1-/- CLP

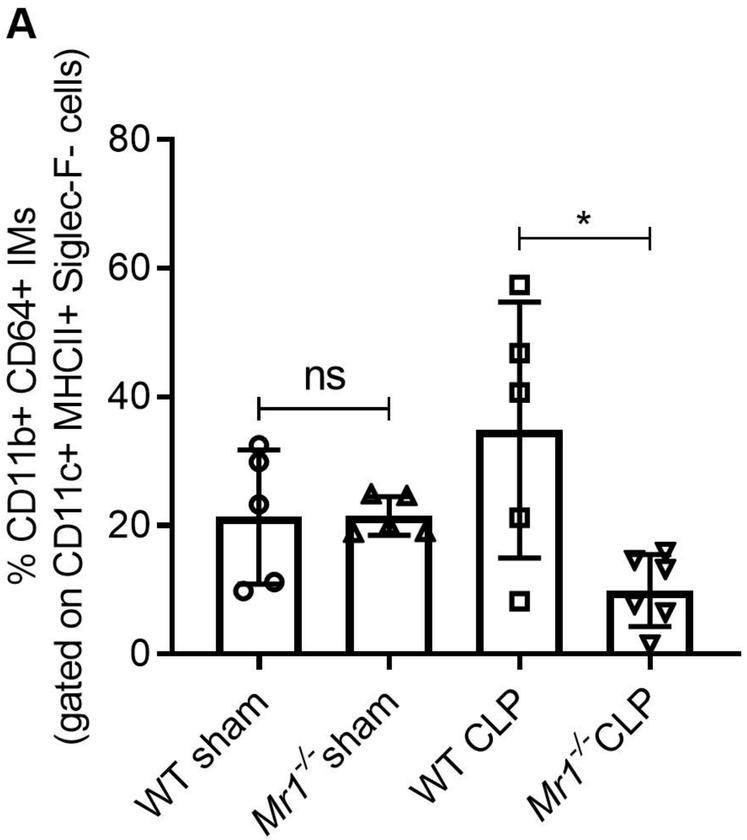
A
% CD11b+ CD64+ IMs
(gated on CD11c+ MHCII+ Siglec-F- cells)
80
60
40
20
0
ns
*
WT sham
Mr1-/- sham
WT CLP
Mr1-/- CLP

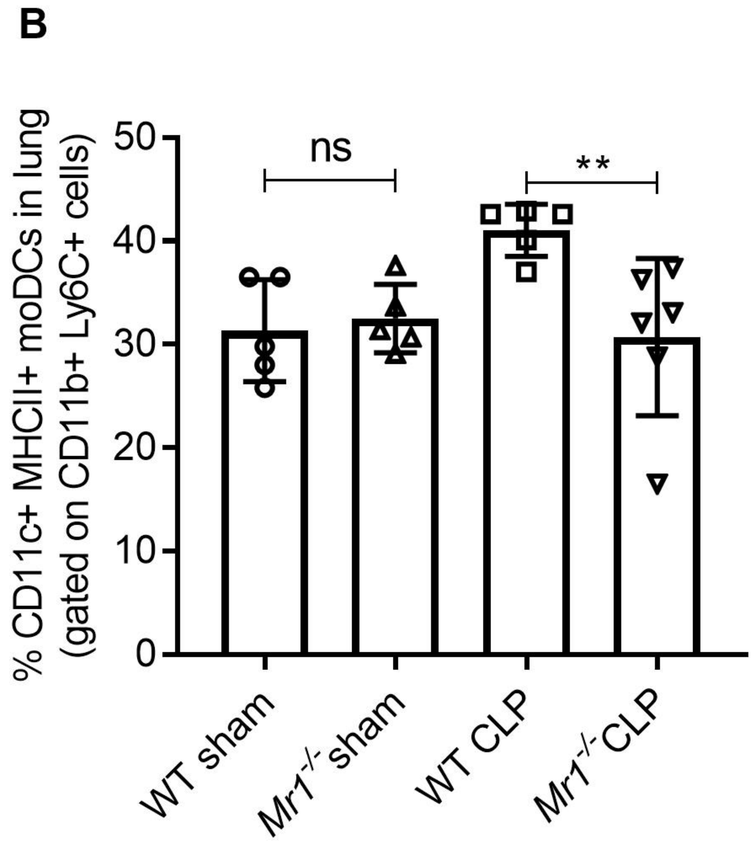
B
% CD11c+ MHCII+ moDCs in lung
(gated on CD11b+ Ly6C+ cells)
50
40
30
20
10
0
ns
**
WT sham
Mr1-/- sham
WT CLP
Mr1-/- CLP

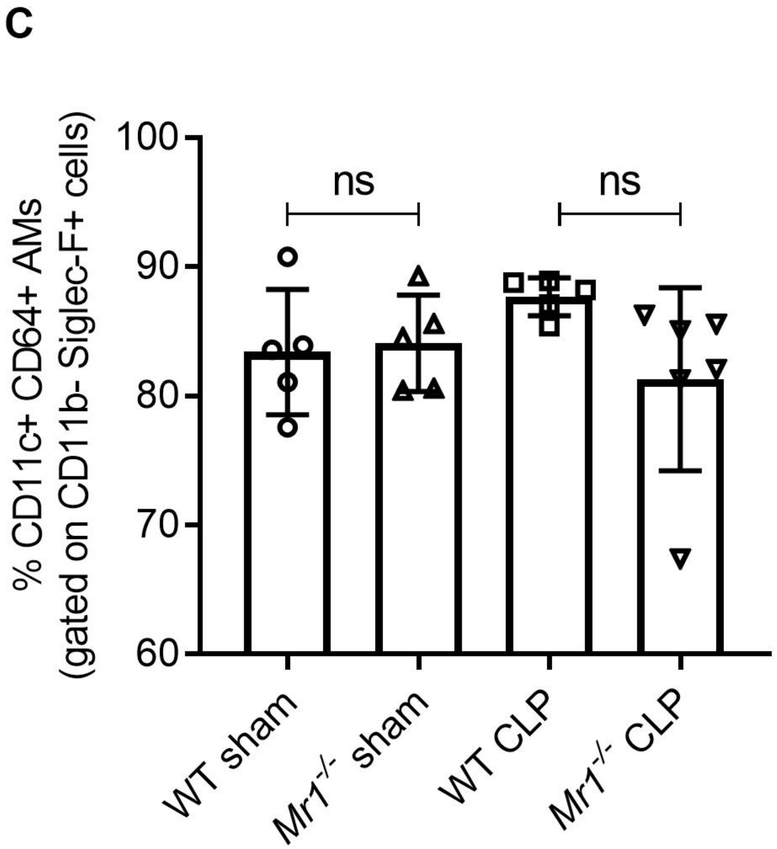
C
% CD11c+ CD64+ AMs
(gated on CD11b- Siglec-F+ cells)
100
90
80
70
60
ns
ns
WT sham
Mr1-/- sham
WT CLP
Mr1-/- CLP

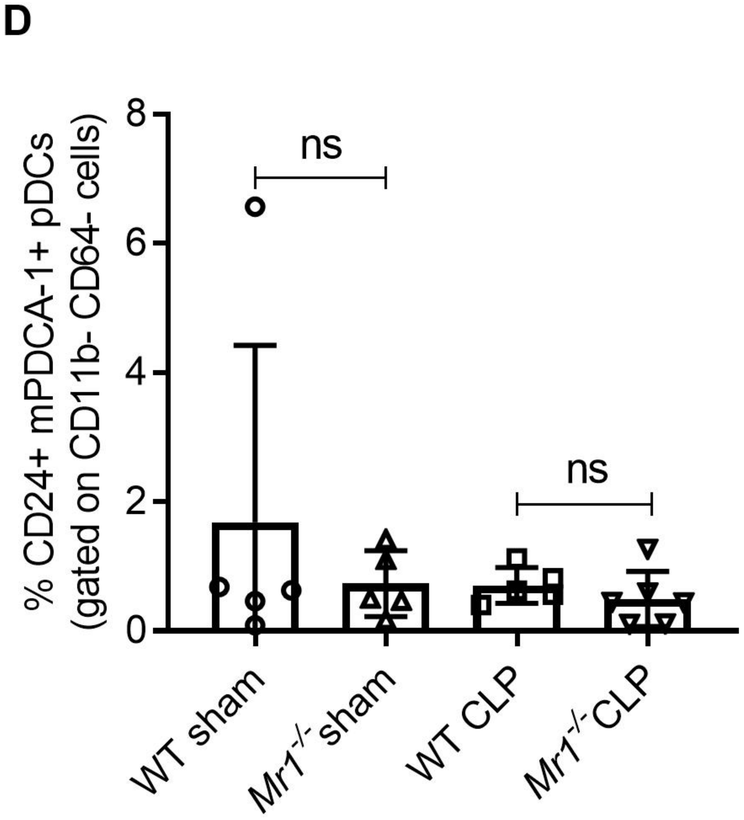
D
% CD24+ mPDCA-1+ pDCs
(gated on CD11b- CD64- cells)
8
6
4
2
0
ns
ns
WT sham
Mr1-/- sham
WT CLP
Mr1-/- CLP

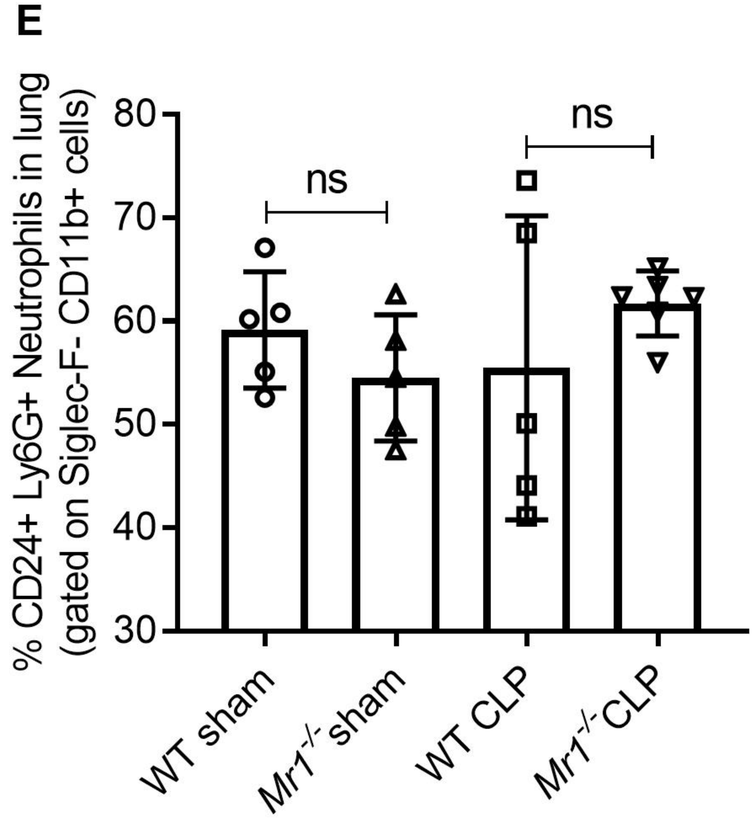
E
% CD24+ Ly6G+ Neutrophils in lung
(gated on Siglec-F- CD11b+ cells)
80
70
60
50
40
30
ns
ns
WT sham
Mr1-/- sham
WT CLP
Mr1-/- CLP

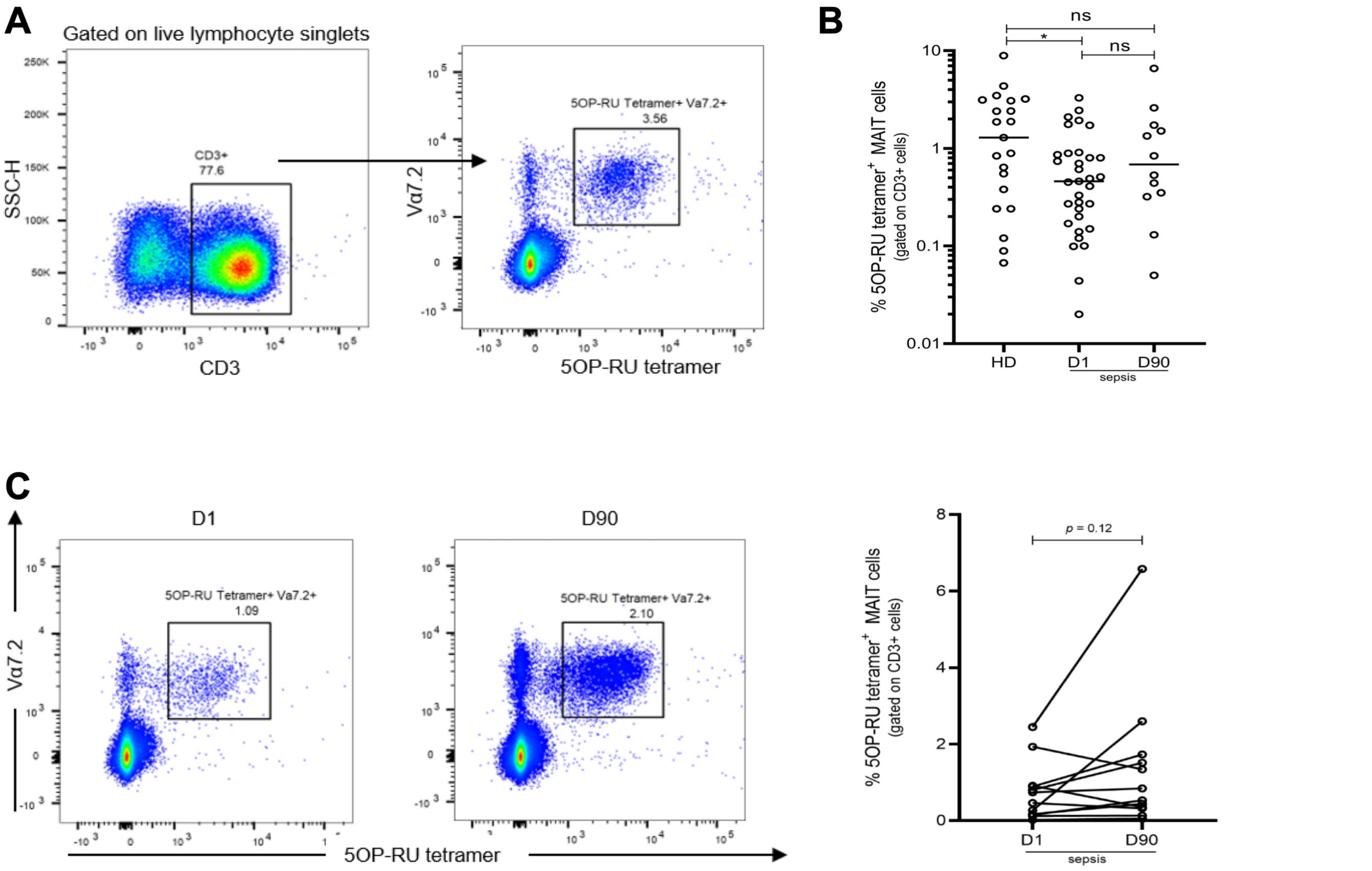
A
Gated on live lymphocyte singlets
CD3+
77.6
SSC-H
CD3
5OP-RU Tetramer+ Va7.2+
3.56
Va7.2
5OP-RU tetramer
B
ns
*
ns
% 5OP-RU tetramer+ MAIT cells
(gated on CD3+ cells)
HD
D1
D90
sepsis
C
D1
D90
5OP-RU Tetramer+ Va7.2+
1.09
5OP-RU Tetramer+ Va7.2+
2.10
Va7.2
5OP-RU tetramer
p = 0.12
% 5OP-RU tetramer+ MAIT cells
(gated on CD3+ cells)
D
HD
D1
D90
CD38
CD69
CD137
HLA-DR
CD38
20.7
CD38
47.6
CD38
35.4
CD69
20.4
CD69
33.1
CD69
10.5
CD137
1.54
CD137
9.68
CD137
2.27
HLA-DR
1.85
HLA-DR
10.5
HLA-DR
8.07
SSC-H
% of MAIT Cells
E
LAG-3 +
TIM-3 +
PD-1 +
% of MAIT Cells

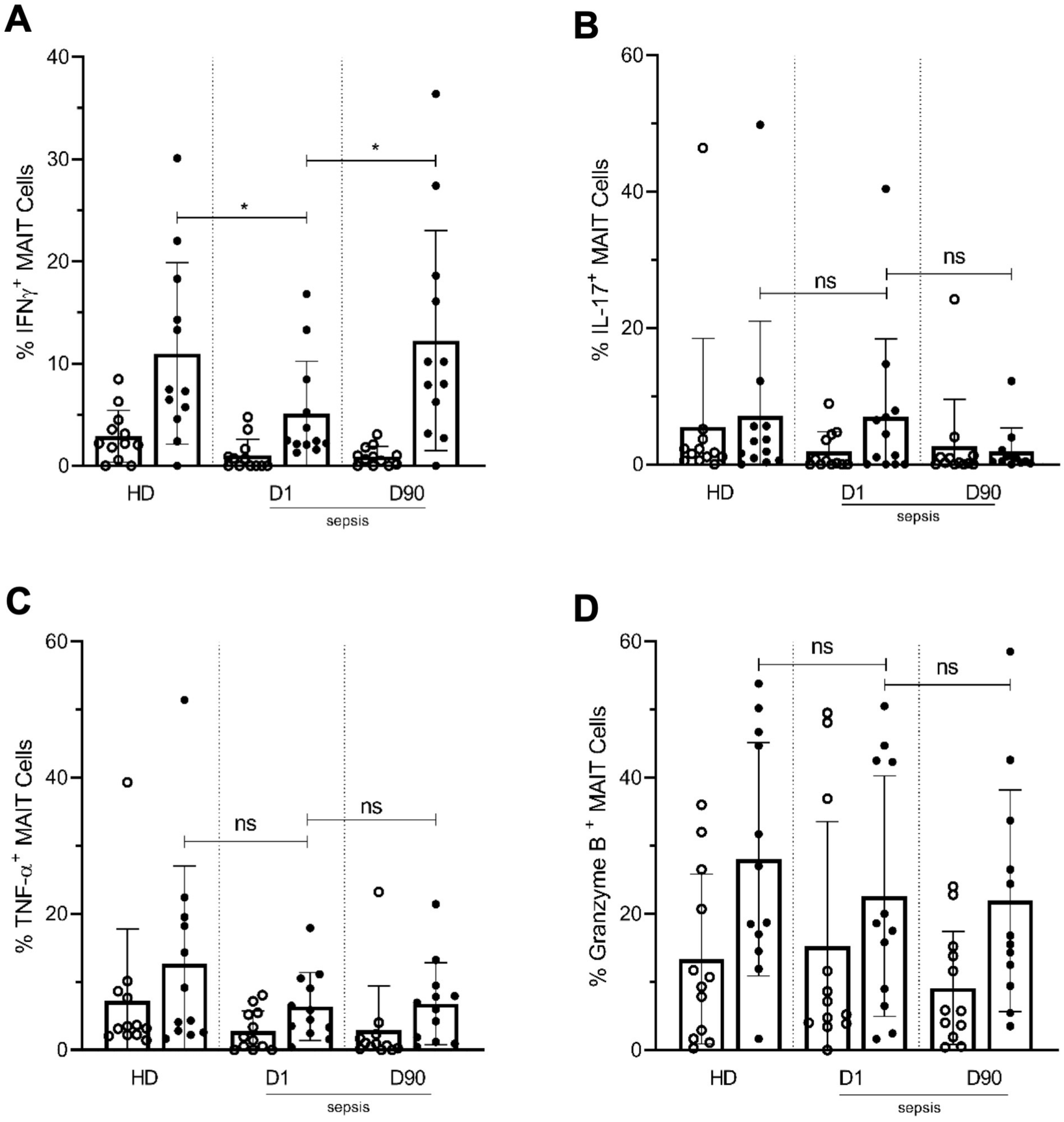
A
% IFNγ+ MAIT Cells
40
30
20
10
0
*
*
HD
D1
D90
sepsis
B
% IL-17+ MAIT Cells
60
40
20
0
ns
ns
HD
D1
D90
sepsis
C
% TNF-α+ MAIT Cells
60
40
20
0
ns
ns
HD
D1
D90
sepsis
D
% Granzyme B + MAIT Cells
60
40
20
0
ns
ns
HD
D1
D90
sepsis

ExPEC

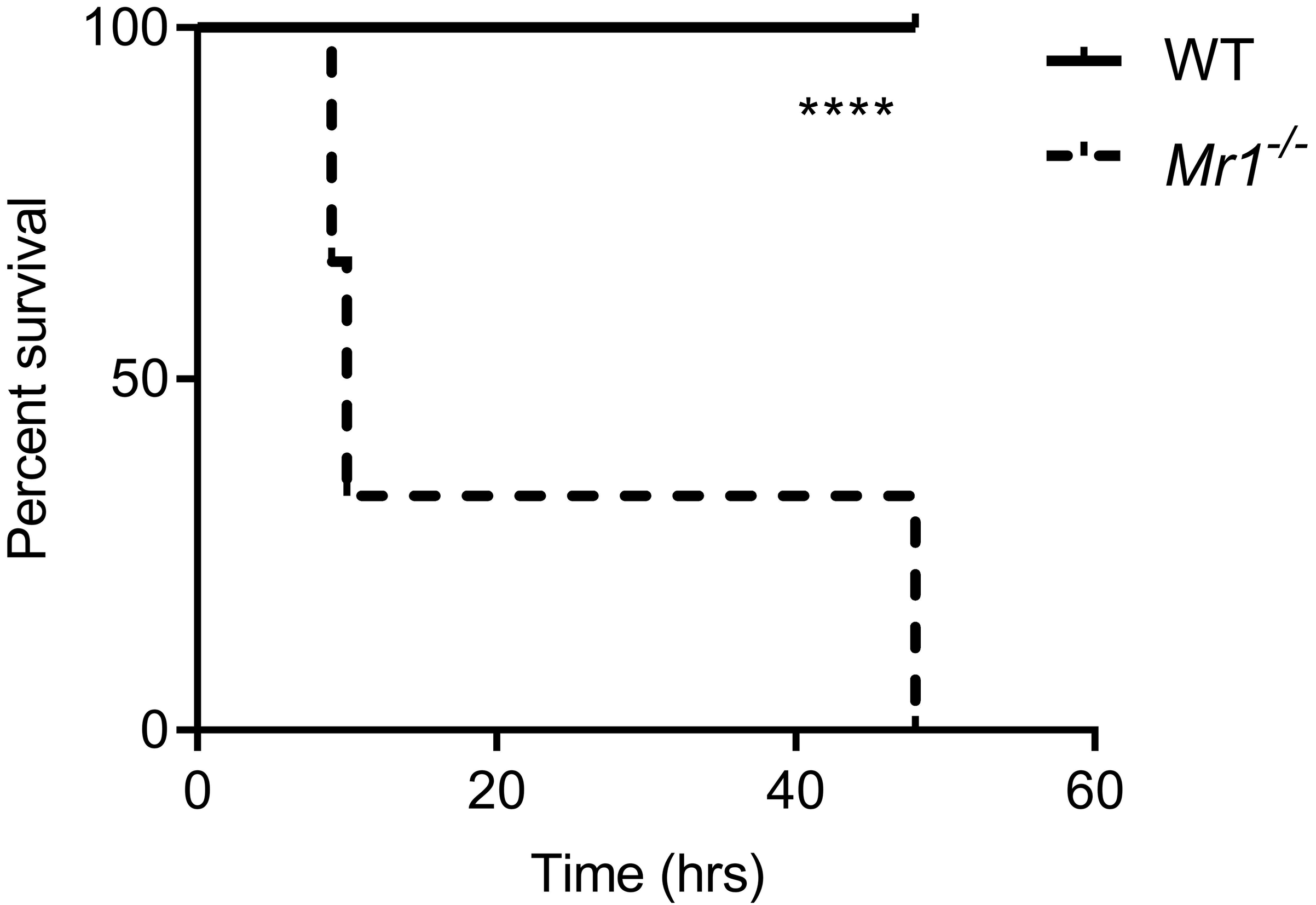

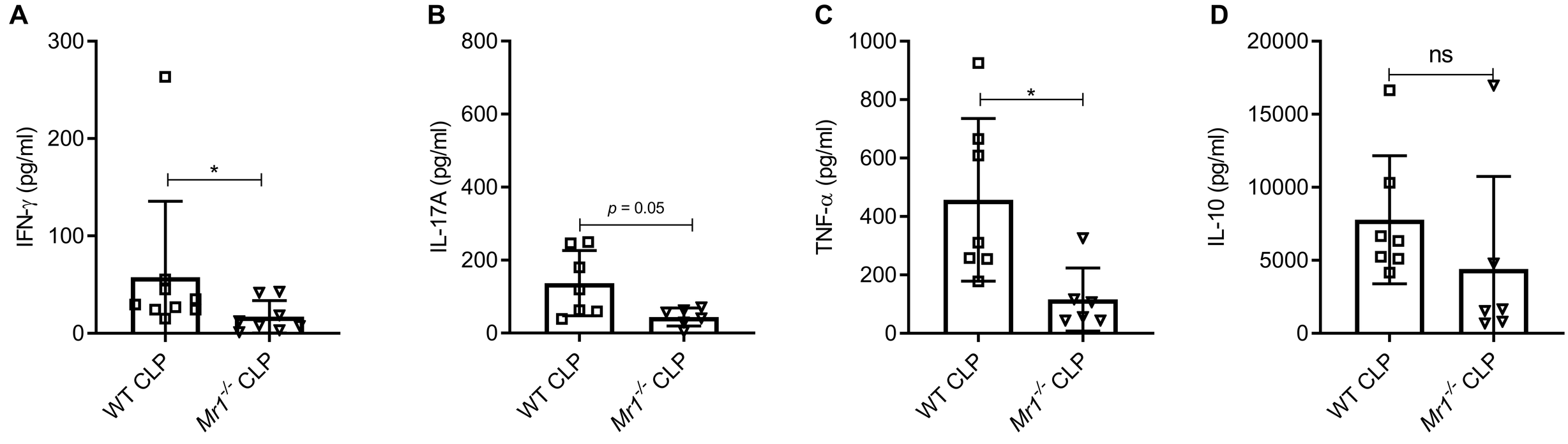
A
IFN-γ (pg/ml)
300
200
100
0
*
WT CLP
Mr1-/- CLP
B
IL-17A (pg/ml)
800
600
400
200
0
p = 0.05
WT CLP
Mr1-/- CLP
C
TNF-α (pg/ml)
1000
800
600
400
200
0
*
WT CLP
Mr1-/- CLP
D
IL-10 (pg/ml)
20000
15000
10000
5000
0
ns
WT CLP
Mr1-/- CLP

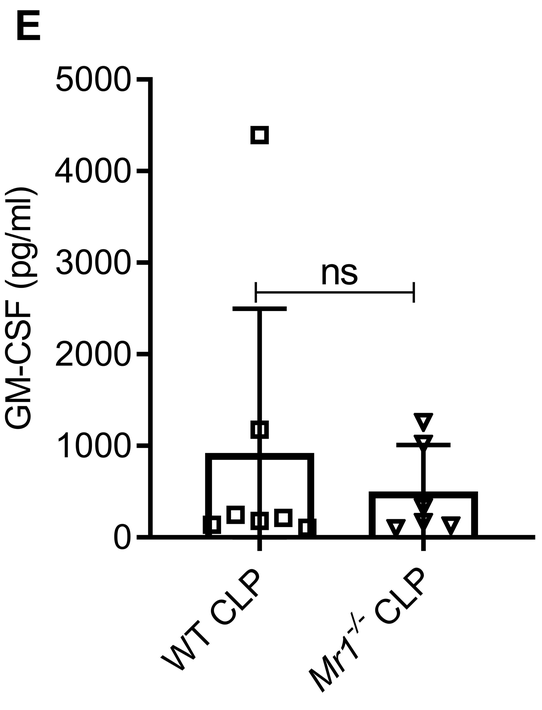
E
GM-CSF (pg/ml)
5000
4000
3000
2000
1000
0
ns
WT CLP
Mr1-/- CLP

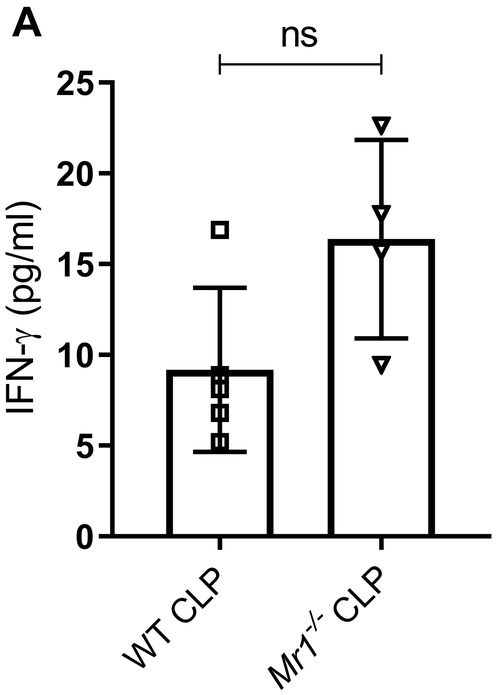
A
ns
IFN-γ (pg/ml)
25
20
15
10
5
0
WT CLP
Mr1-/- CLP

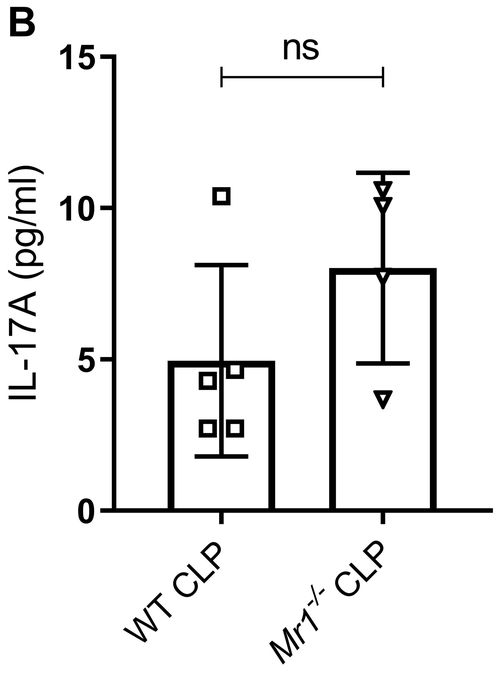
B
ns
IL-17A (pg/ml)
15
10
5
0
WT CLP
Mr1-/- CLP

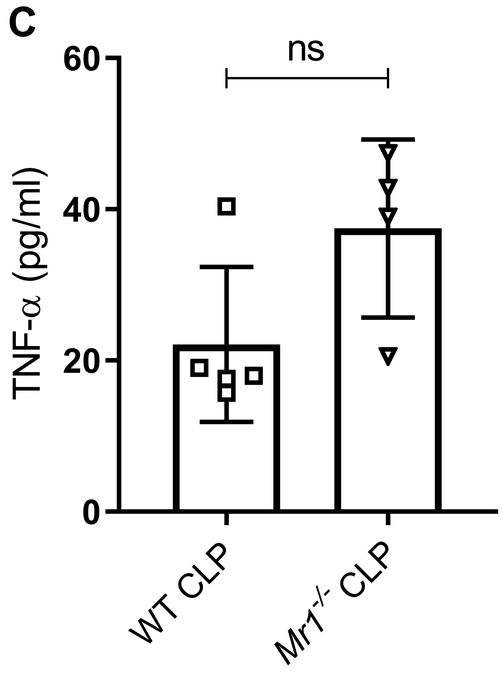
C
ns
TNF-α (pg/ml)
60
40
20
0
WT CLP
Mr1-/- CLP

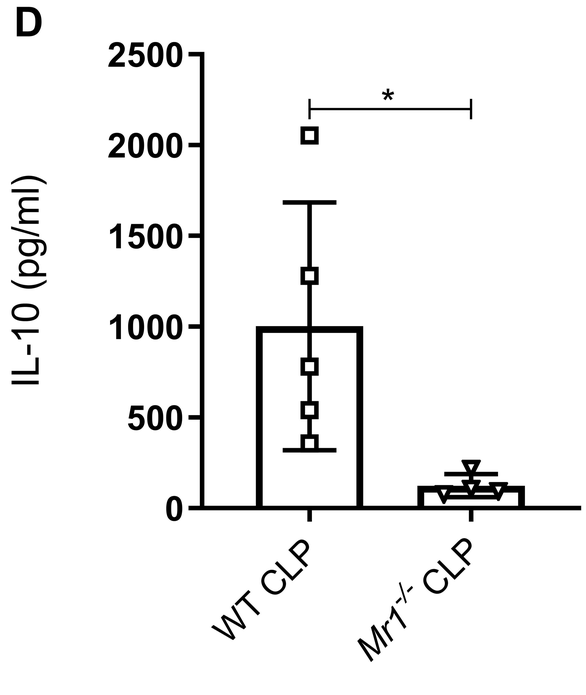
D
*
IL-10 (pg/ml)
2500
2000
1500
1000
500
0
WT CLP
Mr1-/- CLP

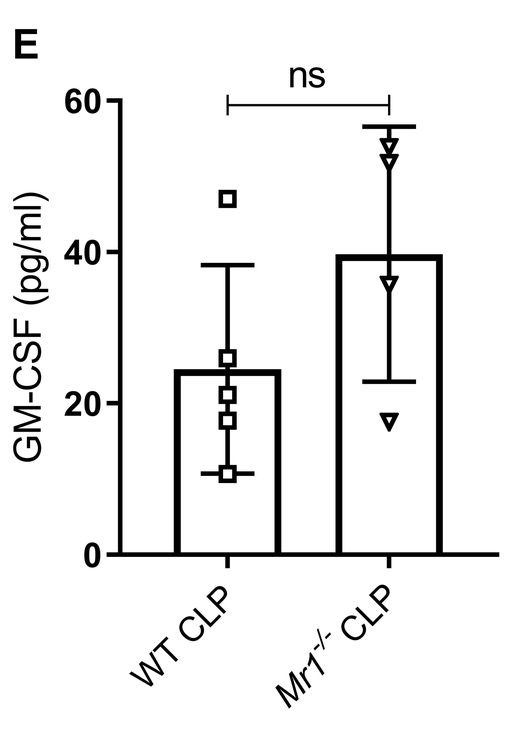
E
ns
GM-CSF (pg/ml)
60
40
20
0
WT CLP
Mr1-/- CLP

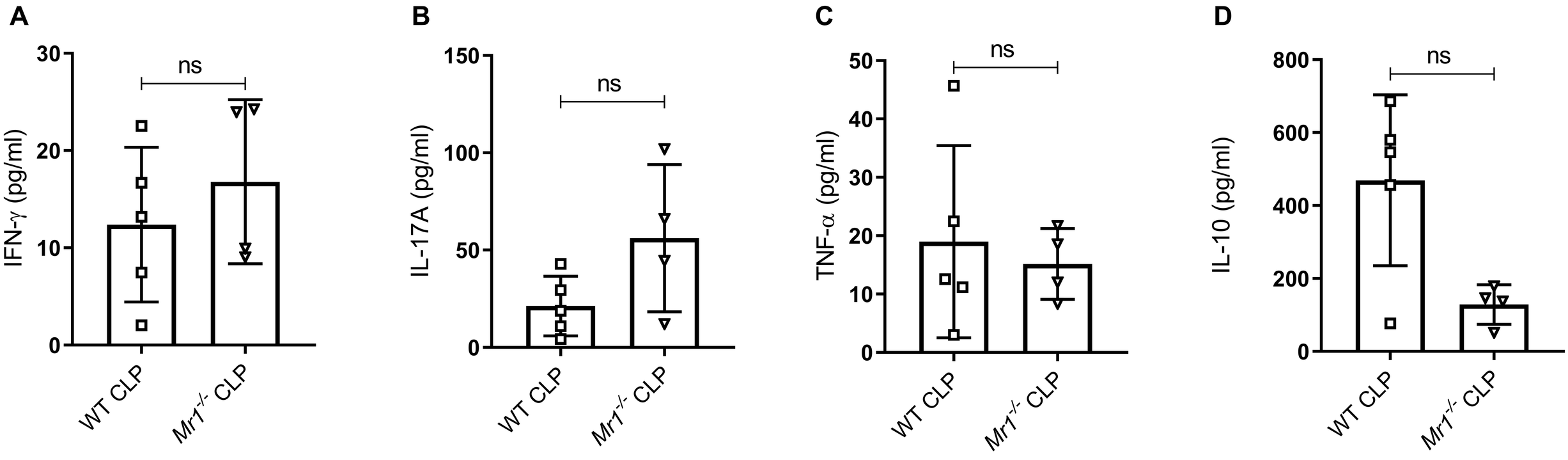
A
IFN-γ (pg/ml)
30
20
10
0
ns
WT CLP
Mr1-/- CLP
B
IL-17A (pg/ml)
150
100
50
0
ns
WT CLP
Mr1-/- CLP
C
TNF-α (pg/ml)
50
40
30
20
10
0
ns
WT CLP
Mr1-/- CLP
D
IL-10 (pg/ml)
800
600
400
200
0
ns
WT CLP
Mr1-/- CLP
E
GM-CSF (pg/ml)
250
200
150
100
50
0
ns
WT CLP
Mr1-/- CLP

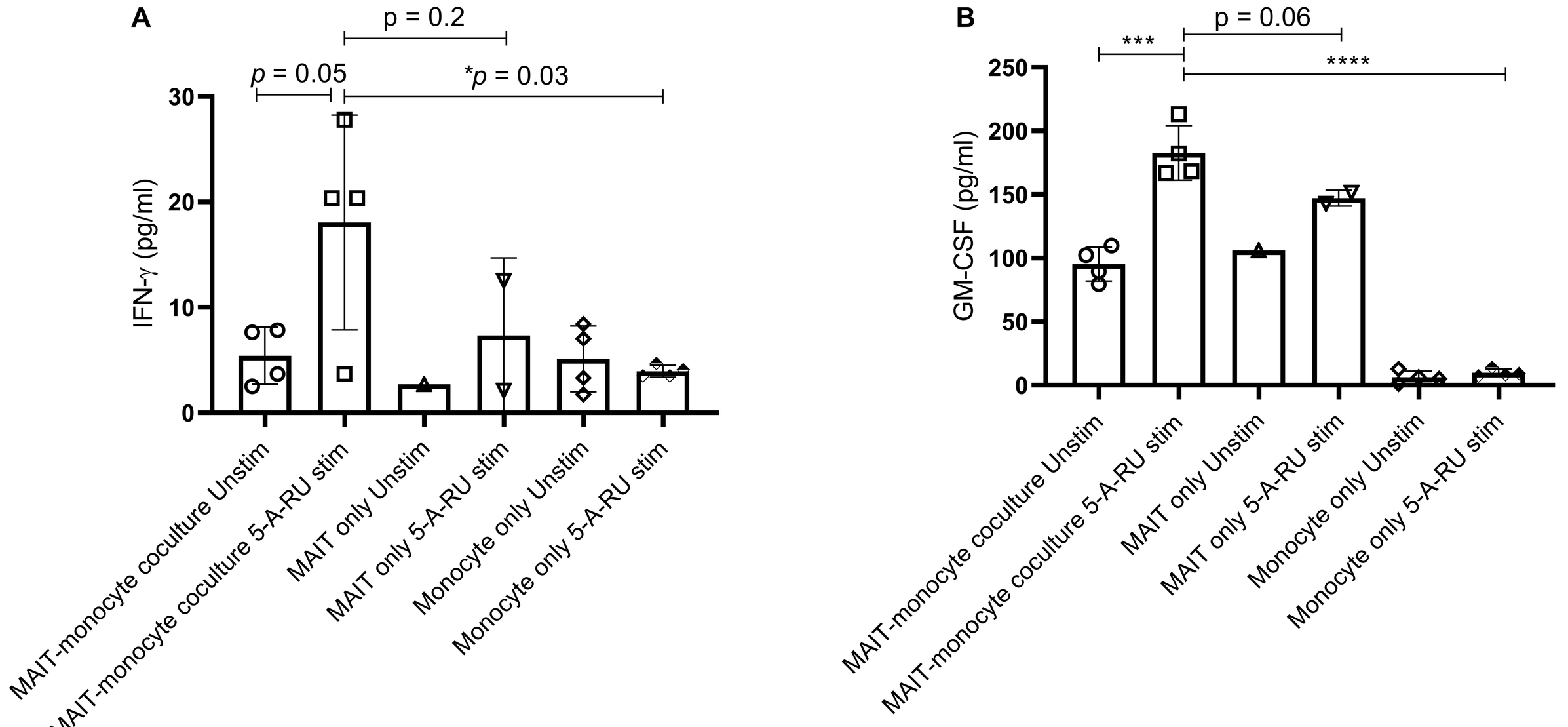
A
p = 0.2
p = 0.05
*p = 0.03
IFN-γ (pg/ml)
30
20
10
0
MAIT-monocyte coculture Unstim
MAIT-monocyte coculture 5-A-RU stim
MAIT only Unstim
MAIT only 5-A-RU stim
Monocyte only Unstim
Monocyte only 5-A-RU stim
B
p = 0.06
***
****
GM-CSF (pg/ml)
250
200
150
100
50
0
MAIT-monocyte coculture Unstim
MAIT-monocyte coculture 5-A-RU stim
MAIT only Unstim
MAIT only 5-A-RU stim
Monocyte only Unstim
Monocyte only 5-A-RU stim

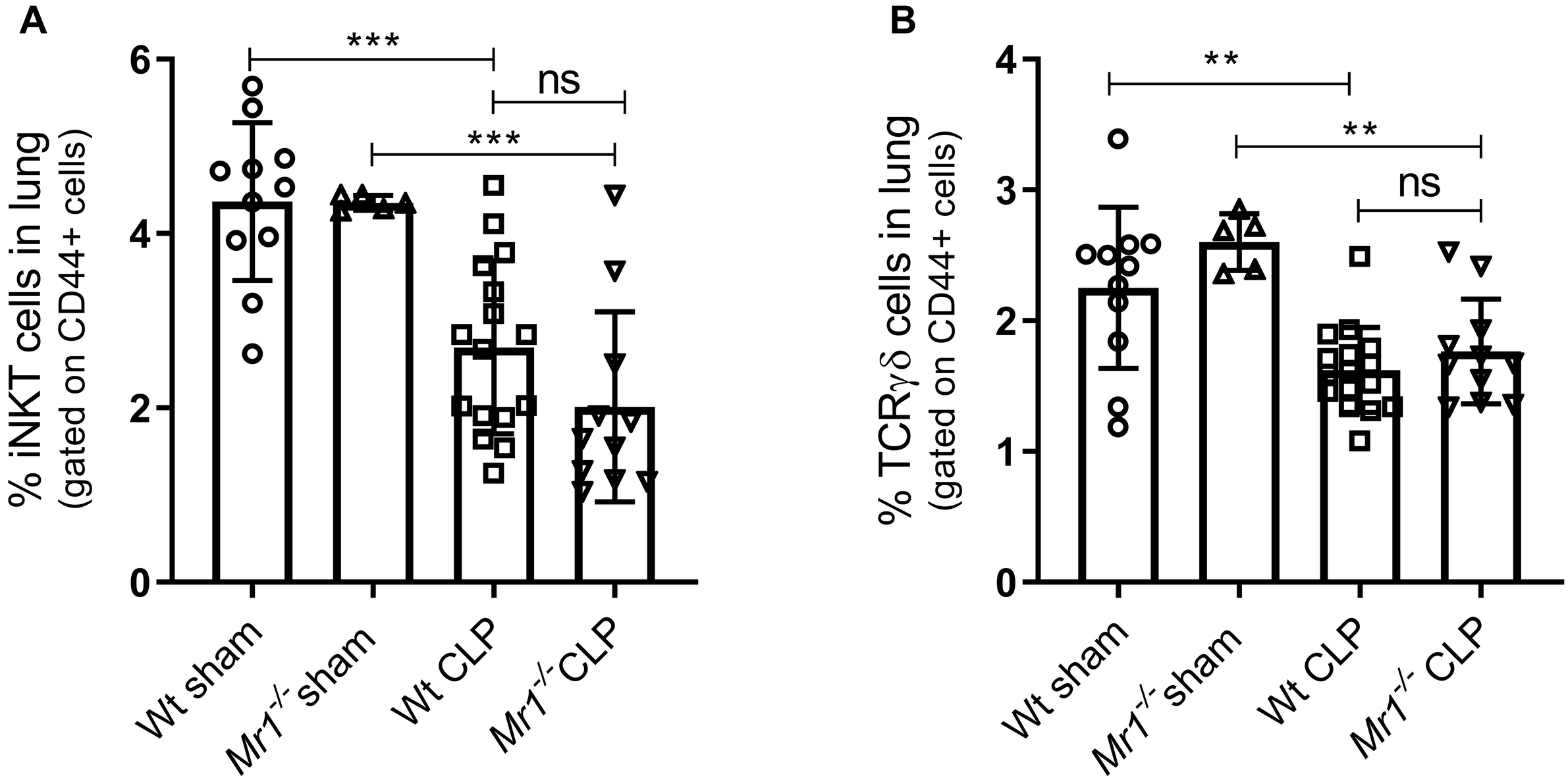
A
% iNKT cells in lung
(gated on CD44+ cells)
6
4
2
0
***
ns
***
Wt sham
Mr1-/- sham
Wt CLP
Mr1-/- CLP
B
% TCRγδ cells in lung
(gated on CD44+ cells)
4
3
2
1
0
**
**
ns
Wt sham
Mr1-/- sham
Wt CLP
Mr1-/- CLP